Eur Biophys J (1993) 22:105–124

European Biophysics Journal

Alamethicin and related peptaibols – model ion channels

M. S. P. Sansom

Laboratory of Molecular Biophysics, The Rex Richards Building, University of Oxford, South Parks Road, Oxford OX1 3QU, UK

Received: 4 February 1993 / Accepted: 4 March 1993

Abstract. Peptaibols are considered as models of those ion channels which consist of a bundle of transbilayer helices surrounding a central pore. X-Ray diffraction and NMR studies have yielded high resolution structures for several peptaibols. In conjunction with other spectroscopic investigations and molecular dynamics simulations, these studies suggest that peptaibols form proline-kinked α-helices, and that there may be "hinge-bending" movement of the helix in the region of the central proline residue. The amphipathicity of peptaibol helices is analyzed in relation to their channel-forming properties. Studies of the interactions of peptaibols with lipid bilayers suggest that they are helical when in a membrane-like environment, and that the helix orientation relative to the bilayer is sensitive to the peptaibol:lipid ratio, and to the degree of hydration of the bilayer. Electrical studies reveal that many peptaibols form multiple-conductance level channels in a voltage-dependent fashion. Analysis of conductance levels provides support for the "barrel stave" model of channel formation, whereby different conductance levels correspond to different numbers of monomers in a helix bundle. Alternative models for voltage-activation are discussed, and the roles of molecular dipoles and of hinge-bending in this process are considered. Two molecular models for an $N = 6$ bundle of alamethicin helices are presented and their electrostatic properties analyzed. The relevance of studies of peptaibols to channel and transport proteins in general is considered.

Key words: Ion channel – Peptaibol – Channel-forming peptide – Molecular modelling

Introduction

The movement of ions through membrane-spanning channel proteins is fundamental to a number of physiological processes, including the electrical properties of excitable cells (Hille 1992). In order to understand this process at the molecular level it is necessary to have atomic resolution structures of channel proteins. However, despite the impressive achievements of cryoelectron microscopy studies of the nicotinic acetylcholine receptor (nAChR; Toyoshima and Unwin 1988; Unwin 1993), such structural information remains elusive for most other ion channels. Channel-forming peptides (CFPs) are model ion channels which mimic many of the functional properties of larger and more complex channel proteins. High resolution X-ray and NMR structures of the monomeric peptides are available, thus offering the possibility of exploring the relationship between channel structure and function at the molecular level.

Ion channels may be formed by bundles of parallel α-helical CFPs (Lear et al. 1988; Sansom 1991), as is illustrated in Fig. 1. The amphipathic helices are oriented perpendicular to the plane of the membrane, and are arranged about a central pore so as to form an assembly with cyclic symmetry about the pore axis. The hydrophilic sidechains of the helices line the central pore, whilst the hydrophobic sidechains interact favourably with the fatty acyl chains of bilayer lipids. Consequently, such assemblies are stabilized by peptide-peptide, peptide-water and peptide-lipid interactions, and also by the interaction of peptide molecular dipoles with the transbilayer electrostatic field.

Parallel bundles of transbilayer α-helices constitute a structural motif present in several ion channel proteins (Oiki et al. 1990). This motif is of particular importance with respect to the members of the nAChR superfamily, the central pores of which are formed by a bundle of five

Abbreviations Aib, α-amino-isobutyric acid; Alm, alamethicin; ATR-FTIR, attenuated total reflection Fourier transform infrared; CD, circular dichroism; CFP, channel-forming peptide; Chol, cholesterol; diPhyPC, diphytanoyl phosphatidylcholine; DMPC, dimyristoyl phosphatidylcholine; DOPC, dioleoyl phosphatidylcholine; DOPE, dioleoyl phosphatidylethanolamine, DPPS, dipalmitoyl phosphatidylserine; DTPC, ditetradecyl phosphatidylcholine, HSM, hydrophilic surface map, I-V, current-voltage; MLV, multilamellar vesicle; nAChR, nicotinic acetylcholine receptor; P:L, protein-to-lipid ratio; POPC, palmitoyloleoyl phosphatidylcholine; SUV, small unilamellar vesicle; Zrv, zervamicin

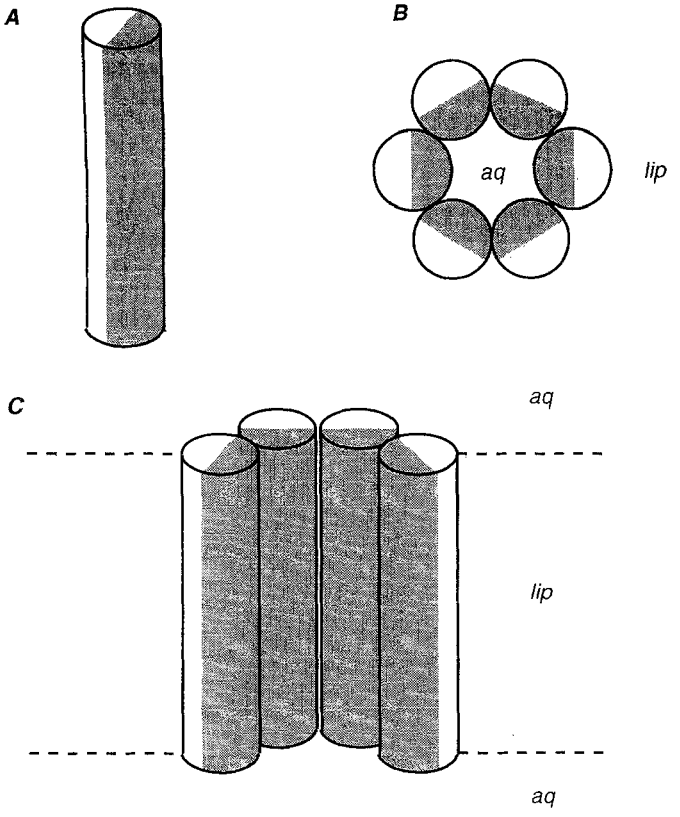

Fig. 1 A–C. Channel formation by a bundle of parallel amphipathic helices. **A** shows a schematic diagram of an amphipathic helix in which the shading represents the hydrophilic surface. **B** shows a hexameric bundle of such helices, viewed down the pore axis. The helices are oriented such that the hydrophilic surfaces form the lining of the pore. **C** shows a section through the helix bundle. Four helices from the hexameric bundle are depicted

parallel amphipathic helices (Unwin 1989, 1993; Stroud et al. 1990; Sansom 1992, 1993). It also may occur in other ion channel proteins. For example, the influenza M_2 channel may be modelled as a bundle of four parallel α-helices (Sansom and Kerr 1993). Helix bundles are also found in channels formed by a number of membrane-active toxins, such as *Bacillus thuringiensis* δ-endotoxin (Li et al. 1991) and *Staphylococcus aureus* δ-toxin (Mellor et al. 1988; Sansom et al. 1991). Furthermore, synthetic peptides designed to form amphipathic α-helices generate cation-selective channels when incorporated into lipid bilayers (Lear et al. 1988).

The proposed transbilayer architecture of voltage-gated channels is somewhat more complex (Bogusz et al. 1992; Durrel and Guy 1992; Miller 1992). It is suggested that the central pore is lined by an eight-strand β-barrel, which in turn is surrounded by an outer bundle of transbilayer helices. There also exist ion channels which do not contain α-helices. In particular, the bacterial porins (Weiss et al. 1991; Cowan et al. 1992) are trimeric transmembrane proteins, each subunit of which is formed by a 16 strand β-barrel. However, in a more general context, bundles of transbilayer helices occur (or are thought to occur) in a wide range of transport proteins. For example, in passing one might consider: (a) bacteriorhodopsin, a photon-driven H^+ pump made of seven helices surrounding a central H^+-conducting "pore" (Henderson et al. 1990); (b) sugar transporters such as lactose permease (Kaback et al. 1990; Marger and Saier 1993), which appear to share a common topology of twelve transbilayer helices; and (c) "ABC"-transport proteins, such as the CFTR (cystic fibrosis transmembrane conductance regulator) and multidrug resistance proteins (which may also act as a Cl^- channels; Wine 1993). It is evident that understanding the nature of transbilayer helix bundles will be of considerable importance with respect to these diverse systems, and therefore it is essential that relevant model systems are investigated in some depth.

The peptaibols are a family of *pep*tides which contain a high percentage of the α,α-dimethyl amino acid α-aminoisobutyric acid (*Aib*) and which have an α-amino alcoh*ol* at the C-terminus. Each peptaibol molecule contains at least one proline residue. Most peptaibols have been isolated from fungal sources, but synthetic analogues have also been investigated. Together, they constitute the most intensively studied example of an ion channel based on the helix bundle motif.

There have been several extensive reviews of peptaibols and related CFPs (Latorre and Alvarez 1981; Sansom 1991; Woolley and Wallace 1992). In this article the focus is on those systems, namely alamethicin and the zervamicins, for which detailed structural information is available. These offer the best possibility of constructing exact molecular models of peptaibol channels in situ. An attempt is made to integrate information from three broad classes of studies: (a) structural studies; (b) studies of peptaibol-bilayer interactions; and (c) investigations of the electrical properties of peptaibol channels. The results from these numerous investigations will be discussed in the context of current models of peptaibol channel formation and structure.

Structural studies

Peptaibol sequences

The sequences of a number of peptaibols for which structural data are available are given in Table 1. Alamethicin (Alm; Padley et al. 1977; Balasubramanian et al. 1981) is 20 residues long and is by far the most intensively investigated peptaibol. The two main forms of alamethicin, Alm-R_f30 and Alm-R_f50 differ only in whether residue 18 is either E or Q respectively. Tricholongin-BI (Rebuffat et al. 1991) and trichorzianine-AIIIC (Le Bars et al. 1988; Duclohier et al. 1989) are 19 residue peptaibols which differ from Alm in the substitution of leucinol or tryptophanol for phenylalaninol at the C-terminus, and of S for G at the position three residues before the central proline. The remaining sequences are for examples of a family of 16 residue peptaibols, the zervamicins (Zrv; Balaram et al. 1992). Note that Zrv-A1-16 is an apolar synthetic analogue of Zrv-Leu and Zrv-IIB (Karle et al. 1987). The zervamicins are of particular interest as high resolution crystal structures for two members of this family are available.

Some important features may be discerned from comparison of the sequences of the peptaibols shown. All are rich in the α,α-dimethyl amino acid Aib. As can be seen

Table 1. Sequences of peptaibols discussed in the text

Peptaibol	Sequence
Alamethicin-R_f30	Ac-U-P-U-A-U-A-*Q*-U-V-U-G-L-U-**P**-V-U-U-*E*-*Q*-F-OH
Alamethicin-R_f50	Ac-U-P-U-A-U-A-*Q*-U-V-U-G-L-U-**P**-V-U-U-*Q*-*Q*-F-OH
L1	Ac-L-P-L-A-L-A-*Q*-L-V-L-G-L-L-**P**-V-L-L-*E*-*Q*-F-NH_2
LL1	Ac-L-P-L-L-A-L-A-*Q*-L-V-L-G-L-L-**P**-V-L-L-*E*-*Q*-F-NH_2
SL1	Ac-*S*-L-P-L-A-L-A-*Q*-L-V-L-G-L-L-**P**-V-L-L-*E*-*Q*-F-NH_2
L2	Ac-L-P-L-A-L-A-*Q*-L-V-L-G-L-L-**P**-V-L-L-*E*-*Q*-F-OH
L3	Ac-L-P-L-A-L-A-*Q*-L-V-L-G-L-L-**P**-V-L-L-*E*-*Q*-W-NH_2
L4	Ac-L-P-L-A-L-A-*Q*-L-V-L-G-L-L-**P**-V-L-L-*Q*-W-NH_2
L2–P2A	Ac-L-A-L-A-L-A-*Q*-L-V-L-G-L-L-**P**-V-L-L-*E*-*Q*-F-OH
L2–P14A	Ac-L-P-L-A-L-A-*Q*-L-V-L-G-L-L-A-V-L-L-*E*-*Q*-F-OH
Tricholongin-BI	Ac-U-G-F-U-U-*Q*-U-U-U-*S*-L-U-**P**-V-U-U-*Q*-*Q*-L-OH
Trichorzianine-AIIIC	Ac-U-A-A-U-U-*Q*-U-U-U-*S*-L-U-**P**-V-U-I-*Q*-*Q*-W-OH
Zervamicin-Leu	Ac-L-I-*Q*-J-I-*T*-U-L-U-***O***-*Q*-U-*O*-U-P-F-OH
Zervamicin-IIB	Ac-W-I-*Q*-J-I-*T*-U-L-U-***O***-*Q*-U-*O*-U-P-F-OH
Zervamicin-A-1–16	BOC-W-I-A-U-I-V-U-L-U-**P**-A-U-P-U-P-F-OMe

Sequences are indicated using the standard one letter abbreviations for amino acids, with the following additions: – J = *D*-isovaline; O = hydroxyproline; and U = α-amino-isobutyric acid. Abbreviations for terminal groups are: – Ac = acetyl; Boc = *t*-butoxycarbonyl; OH = C-terminal amino alcohol; OMe = C-terminal methyl ester; NH_2 = C-terminal amide. Polar residues are indicated by *italic* type. The central, kink-inducing proline (or hydroxyproline) residues are indicated by **bold** type

from Table 1, if the sequences are aligned at their C-termini, then P14 of Alm is conserved (albeit as hydroxyproline in Zrv-Leu and Zrv-IIB). Similarly Q7 of Alm is conserved in all except Zrv-A1-16. Finally, in all the naturally-occurring peptaibols the N-terminus is blocked with an acetyl group and the C-terminal residue is an α-amino alcohol.

α-Aminoisobutyric acid

The conformational freedom of Aib is severely limited to regions, $(\phi,\psi) = \pm(57°, 47°)$ (Burgess and Leach 1973; Balaram 1992). This results in promotion of helical conformations in Aib-containing peptides. Crystal structures are known for ca. 30 synthetic Aib-rich peptides (Karle and Balaram 1990; Karle 1992). Analysis of these structures revealed that the 3_{10} conformation is preferred by peptides of less than ca. 8 residues, whilst the α-helical conformation is preferred by longer peptides. One of the longest 3_{10} helices is that of *p*BrBz-$(Aib)_{10}$-O*t*Bu (Toniolo and Benedotti 1991). These authors have also demonstrated a 3_{10} helix sub-type, the β-bend ribbon, in *p*BrBz-Aib-$(Pro\text{-}Aib)_3$-OMe. As discussed below, this is of particular interest with respect to the C-terminal segment of the zervamicins, which contain alternating Aib and Pro (or hydroxy-Pro) residues.

The factors determining the "transition" from 3_{10}- to α-helix (i.e. from $(\phi,\psi) = (-57°, -30°)$ to $(-63°, -42°)$; Toniolo and Benedetti 1991) are of interest when considering possible conformations of peptaibols in membrane (i.e. hydrophobic) environments. Marshall et al. (1990) performed molecular mechanics calculations to compare the 3_{10}- and α-helical conformations of Aib_N (N = 1–15). They concluded that the α-helix was inherently more stable than the 3_{10}-helix by ca. 2 kcal/mol/residue. This is because the intrahelical H-bond is non-linear in the 3_{10}-helix, and hence is less stable. However, a 3_{10}-helix has one more H-bond/residue than an α-helix, and so there is a "transition length" below which the former conformation is preferred. The transition is dependent, *inter alia*, on the solvent polarity, with more polar solvents favouring the α-helix. Molecular mechanics calculations by Aléman et al. (1992) on Aib_{12} suggested that the transition length for $3_{10} \rightarrow \alpha$ depended on the dielectric model used in evaluation of electrostatic energies. Thus the transition length was 12 for $\varepsilon = 1$; 7 for $\varepsilon = 1$ r; and 3 for $\varepsilon = 4$ r. Overall, it seems that the exact conformation of short Aib-rich helices may be sensitive to the environment surrounding a peptaibol.

Crystal structures

High resolution crystal structures have been determined for alamethicin-R_f30 (crystallized from acetonitrile/methanol, data to 1.5 Å resolution, Fox and Richards 1982), zervamicin-A-1-16 (methanol/water, 0.9 Å, Karle et al. 1987), zervamicin-Leu (methanol/water, polymorph A 0.9 Å, Karle et al. 1991; polymorph B 1.1 Å, Karle et al. 1992), and trichorzianine AIIIC (0.9 Å, Le Bars et al. 1988). These studies have provided a wealth of information for understanding of the properties of peptaibol CFPs.

There are three independent alamethicin molecules in the asymmetric unit. Overall, their structures resemble one another quite closely. The structure of monomer A is shown in Fig. 2A. The molecule is α-helical with a kink induced by P14. The polar sidechains lie on the convex face of the kinked helix (see below). The kink angle varies slightly between the three monomers (39° for monomer A, 35° for monomers B and C; R. Sankararamakrishnan, personal communication). Analysis of the pattern of H-bonding of Alm reveals that there is a 4→1 H-bond from V15 to L12. Furthermore the carbonyl residues of U10 and G11 do not form intramolecular H-bonds but instead interact with the solvent. The carbonyl oxygen of

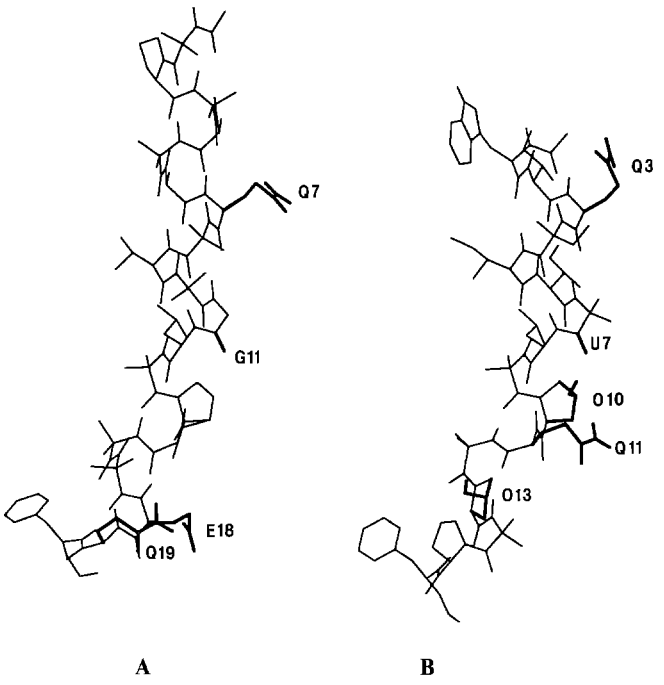

Fig. 2 A, B. Peptaibol structures. **A** shows the crystal structure of Alm-R_f30 (monomer A). Sidechains Q7, E18 and Q19, and the carbonyl group of G11 are highlighted. **B** shows a model structure for Zrv-IIB, derived from the crystal structure of Zrv-Leu Sidechains Q3, O10, Q11 and O13, and the carbonyl group of U7 are highlighted

G11 is particularly solvent exposed. Thus the central kink locally disrupts the 5→1 H-bonding pattern and exposes the peptide backbone.

The backbone structures of the zervamicins are all similar. In each case a kinked helical structure is formed, similar to that for alamethicin. The N-terminal helix (i.e. up to residue P10 or O10) is α-helical. The C-terminal helix is distorted away from α-helical geometry by the presence of additional proline (or hydroxyproline) residues. The helix thus formed is a β-bend ribbon. As discussed above, this is also seen in *p*BrBz-Aib-(Pro-Aib)$_3$-OMe (Toniolo and Benedotti 1991). A model of the structure of Zrv-IIB, based on the crystal structure of polymorph A of Zrv-Leu (Sansom et al. 1993) is shown in Fig. 2B. As with Alm the polar sidechains are located on the hydrophilic face of the kinked helix, and the carbonyl oxygen preceding the kink (that of U7) is exposed to the solvent as a result of disruption of the 5→1 H-bonding pattern. The kink angle of Zrv-Leu varies, from 30° to 45°, with the water content of the four polymorphs (Karle et al. 1992).

The structure of trichorzianine AIIIC has been reported in abstract form (LeBars et al. 1988). As with the other peptaibols, trichorzianine forms a kinked helix with the polar residues on the convex face of the molecule. Further details of this structure are eagerly awaited.

It is worth commenting on the variation in the helix kink angle induced by the central proline in peptaibol molecules. Barlow and Thornton (1988) and Sankararamakrishnan and Vishveshwara (1992) have analyzed the kink angle for proline-kinked helices in globular proteins. Both studies arrive at a mean kink angle of 25°. Kink angles varied from 9° to 49°. Interestingly, the largest kink angle is for the non-peptaibol CFP melittin, which shares many functional and structural properties with alamethicin (Dempsey 1990).

A further property in common of alamethicin and the zervamicins is their amphipathicity. This may be seen directly from their structures as shown in Fig. 2. One may also attempt to quantify amphipathicity. This may be achieved by evaluation of the potential energy of interaction of a water molecule located at different positions on the surface of a peptaibol molecule, resulting in a hydrophilic surface map (HSM). If the water molecule positions are defined according to a cylindrical polar coordinate system, with the cylinder axis coincident with the helix axis, then the HSM may be readily displayed superimposed on a helical net representation of the Cα coordinates (Sansom and Kerr 1993). The results of such HSM analysis for models of Alm-R_f50 and Zrv-IIB are shown in Fig. 3. The Alm-R_f50 model was based on the crystal structure of Alm-R_f30 (monomer B), "mutating" E18Q and using energy minimization to optimize the conformation of the Q18 sidechain. The Zrv-IIB model was that described above.

For alamethicin-R_f50 (Fig. 3A), HSM analysis reveals hydrophilic surface patches at the N-terminus, in the regions of polar sidechains Q7, Q18 and Q19. There is also a hydrophilic region between G11 and P14 which is due to the exposed carbonyl oxygen of the former residue. For Zrv-IIB a similar pattern is observed, with hydrophilic patches in the vicinity of the polar sidechains of Q3, O10, Q11 and at the C-terminus. There is also a hydrophilic patch due to the exposed carbonyl of U7. For both Alm and Zrv, the hydrophilic patches lie predominantly on one face of the helix, confirming the amphipathicity suggested by visual examination of their structures.

NMR and dynamics

There have been several NMR studies of peptaibols, principally of alamethicin, which provide valuable information on the structure and dynamics of these peptides when in isotropic solution. Banerjee et al. (1983) used ^{1}H NMR to examine the structure of Alm-R_f30 in methanol, water and methanol/water solutions. They concluded that the N-terminal half of the molecule was α-helical but that the C-terminal region adopted an extended β-strand conformation. The latter conclusion was not supported by the more detailed ^{1}H NMR study by Esposito et al. (1987), again of Alm-R_f30 in solution in methanol. They concluded that the solution structure was essentially the same as in the crystal, except that the C-terminal dipeptide was somewhat more extended. The conformation was insensitive to the protonation state of E18.

Recent NMR studies have focused on the possibility of "hinge-bending" motions of the kinked Alm helix. Yee and O'Neil (1992) carried out ^{1}H and ^{15}N NMR studies on ^{15}N-labelled Alm-R_f50 in methanol. They concluded that the region form U3 to G11 was helical, whereas the

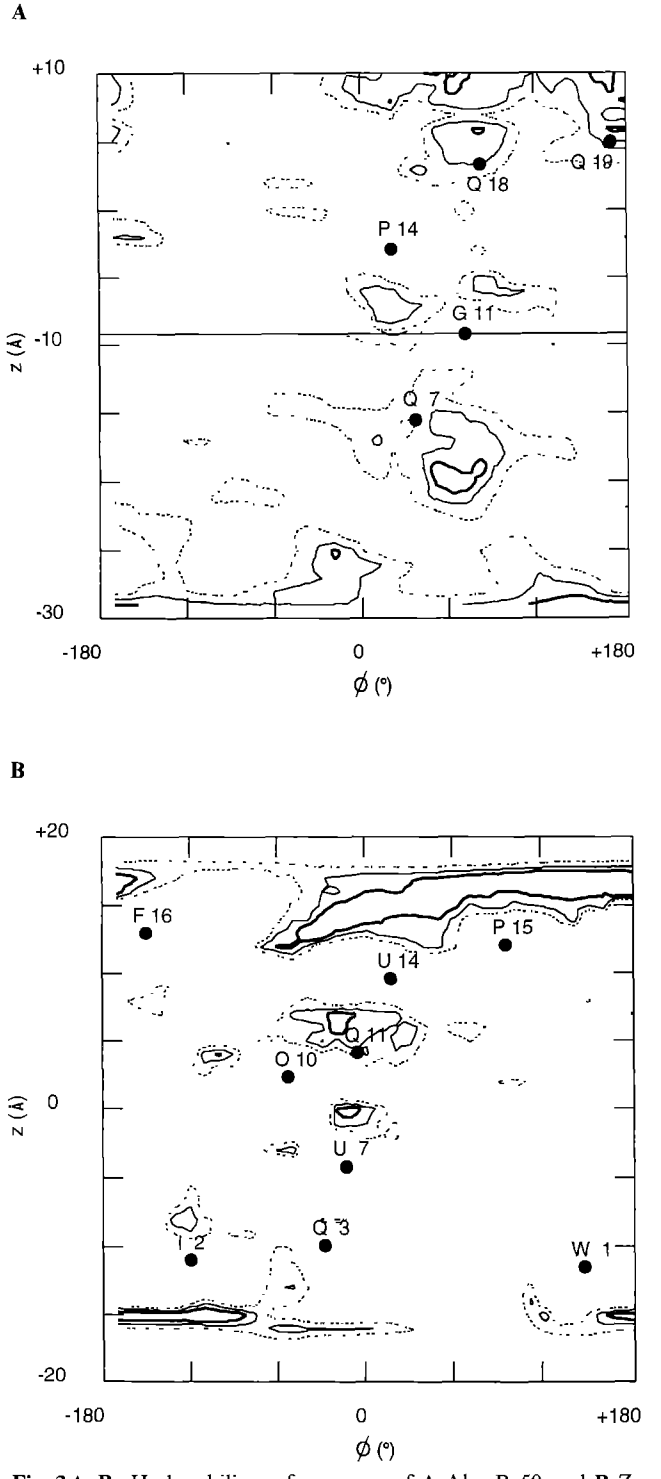

Fig. 3A, B. Hydrophilic surface maps of **A** Alm-R_f50 and **B** Zrv-IIB. In both cases the maps show the interaction energy of a water molecule probe with the surface of the peptaibol molecule as a function of distance along the helix axis (z) and of angle about the helix axis (ϕ). The helices run from negative z values (N-termini) to positive z values (C-termini). Isopotential contours are shown for interaction energies of -4 (*dotted lines*), -6 (*solid lines*) and -8 (*bold lines*) kcal/mol. The positions of the Cα atoms of selected sidechains are superimposed on the maps. In the case of Alm-R_f50 the helix kink necessitated the calculation of the surface map in two halves, one for the N-terminal segment and one for the C-terminal segment. The "join" between the two halves is indicated by the horizontal line at z=ca. -10 Å

region from L12 to F20 was less well defined in their studies, possibly as a result of there being fewer NOEs and coupling constants for this region. There was a suggestion of conformational averaging at L12 and V15. They interpreted these data in terms of possible conformational variation in the C-terminal region. However, heteronuclear NOE measurements did not confirm a variation in dynamics along the length of the peptide. A similar conclusion was arrived at by Kelsh et al. (1992) on the basis of ^{13}C NMR studies of Alm-R_f50 in methanol. They demonstrated that the T_1 derived order parameter for the Cα atoms showed little variation along the length of the molecule. This suggests that alamethicin behaves as a rigid helical rod, at least on a fast (ca. 1 ps) timescale. Furthermore, T_2 measurements provided no evidence for slower motions modulating the alamethicin conformation.

A detailed study of the structure and dynamics of a 19 residue peptaibol, tricholongin-B, has been provided by Rebuffat et al. (1991), from ^{1}H and ^{13}C NMR studies in methanol. The results provided evidence for a helical structure, with a kink in the region of P13. The ^{13}C T_1 measurements suggested that this peptaibol also had "an uniformly rigid peptide backbone on the timescale of molecular tumbling".

However, the picture of peptaibols behaving as rigid helical rods is less clear once one takes into account the results of molecular dynamics simulations. Fraternali (1990) carried out extensive dynamics simulations of Alm, starting from the crystal structure and incorporating restraints derived from the NMR data of Esposito et al. These simulations suggested that the molecule could be divided into three regions, region A from U1 to V9, region B from U10 to G11, and region C from L12 to F20. Region B appeared to act as a "hinge" region between A and C, the latter two regions behaving as relatively rigid helical rods. Dynamics simulations of two related (non-peptaibol) proline kinked helices support this conclusion. Pastore et al. (1989) carried out molecular dynamics simulations of melittin, based on the ^{1}H NMR derived structure determination of this peptide in methanol. In a restrained dynamics run, the kink angle between the N- and C-terminal helices fluctuated between ca. 5° and 45° on a 10 ps timescale. Substitution of P14 by alanine results in loss of the hinge bending motion (Dempsey et al. 1991). A similar dynamic behaviour of a proline kinked helix was seen by Sankararamakrishnan and Vishveshwara (1993) for a simplified model of helix F from bacteriorhodopsin. Again hinge bending motions were observed, with the kink angle varying between 0° and 50°, on a 10 ps timescale. Replacement of the central proline by alanine resulted in loss of the bending motion.

Overall, the following picture of peptaibol structure emerges. A range of peptaibols have been shown to form amphipathic kinked helices. Comparison of crystal structures suggests that static conformational variation in terms of the kink angle may occur, as is seen in a range of globular proteins. NMR studies confirm that the same overall structure is seen in solution. However, there is some dispute over the timescale of hinge bending motions. Dynamics simulations suggest that these occur on

a 10 ps timescale. However, NMR measurements which should be capable of detecting motions on this timescale fail to provide experimental evidence. This discrepancy remains to be resolved.

Peptaibol-bilayer interactions

Clearly, in order to understand the channel-forming properties of peptaibols one should take into consideration interactions with the lipid bilayer environment. In particular, it is necessary to consider possible effects of lipid bilayers on peptaibol conformation, and also the orientation of the peptaibol molecule relative to the bilayer plane. A further consideration is that of the aggregation state of bilayer associated peptaibols.

In interpreting the results of studies of peptaibol-bilayer interactions it is important to note that in many cases the molar ratio of peptide to lipid ($P:L$) is much higher than that present in functional (i.e. electrophysiological) studies of peptaibol channels.

Bilayer effects on peptaibol conformation

There are several spectroscopic studies of the structure of alamethicin in different environments. Circular dichroism (CD) studies suggest a largely α-helical structure, with the estimated percentage helicity dependent on the solvent system used. For example, studies of alamethicin in dioxane/octanol mixtures suggest that the percentage helicity increases with the percentage of octanol in the solvent (Schwarz et al. 1983).

Fourier transform infra-red studies of alamethicin have been carried out by Haris and Chapman (1988), comparing alamethicin spectra with those of bacteriorhodopsin. Alamethicin spectra were collected for alamethicin in a KBr disk, in methanol and in the presence of an aqueous lipid dispersion. In all three cases the spectra were similar to those obtained from bacteriorhodopsin, suggesting that the peptaibol is largely α-helical in a range of environments.

A detailed combined CD and Raman spectroscopy investigation of alamethicin has been carried out by Vogel (1987). Reviewing earlier studies this author suggested that CD measurements underestimated the helical content of alamethicin (in methanol). From analysis of the amide I band in the Raman spectrum of alamethicin in methanol, it was concluded that the secondary structure composition was 31% α-helix and 29% disordered helix (which includes 3_{10} helix), yielding an overall helicity of 60%. The conformation DMPC and DTPC vesicles ($P:L=1:20$) was also measured. It was evident that the degree of helicity of alamethicin increased upon interaction with the bilayer above that observed in the absence of lipid (in methanol), provided that the temperature was below T_c for the lipid. For example, from analysis of the Raman spectra of alamethicin in methanol, in DMPC vesicles at 15 °C ($<T_c$) and in DMPC vesicles at 33 °C ($>T_c$), the percentage helicities were, respectively, 60, 74 and 58%. A similar conclusion was reached on the basis of CD studies by Cascio and Wallace (1988) who showed an increase in helicity in DMPC SUVs to a value comparable to that found in the crystal.

All of the above spectroscopic studies indicate that the secondary structure of alamethicin becomes more defined in the presence of lipid bilayers. However, relative to studies of alamethicin channel (see below), there is something absent from these investigations, namely the transbilayer potential. Brumfeld and Miller (1990) employed polyelectrolytes in order to impose a Donnan potential across the bilayer of lipid vesicles which were exposed to alamethicin on their exterior face. CD measurements indicated an increase in helical content when the outside of the vesicles was made positive relative to the inside, and a decrease in helical content when the voltage was reversed. This suggests that the conformation of alamethicin is sensitive to changes in the transbilayer electrostatic field.

Helix orientation with respect to the bilayer

In order to develop models of channel formation, it is essential to have information on the orientation of peptaibol helices relative to the bilayer. The results of several spectroscopic studies of this problem are quite complex, and require careful consideration if a clear picture is to emerge.

Banerjee et al. (1985) used ^{31}P to show that alamethicin ($P:L=1:15$) perturbed the headgroups of DMPC MLVs. In the same study, both ^{2}H NMR and Raman spectroscopic measurements failed to detect any effect of peptaibol on segmental order of acyl chains of the hydrophobic region of the bilayer. Only those atoms of the acyl chains immediately adjacent to the glycerol backbone had their ^{2}H spectrum perturbed. These results suggests a predominantly interfacial location for alamethicin.

More recent studies have focused on the spectroscopic properties of the peptaibol *per se* when in the presence of planar lipid bilayers. Vogel (1987) used CD spectroscopy to determine the orientation of alamethicin in glass-supported planar multilayers of DTPC ($P:L=1:100$). With hydrated (30% water w/w) multilayers the orientation of the helix is dependent upon the temperature relative to the phase transition temperature of the lipid. Below the transition temperature the helices lie approximately parallel to the bilayer plane. Above the transition temperature, they lie parallel to the bilayer normal. With dry (2% water w/w) membranes the helices lie parallel to the bilayer normal even at the lower temperature. These results may be compared with those of Frey and Tamm (1991), who employed polarised ATR-FTIR to compare the orientation of melittin in hydrated *single* planar bilayers and in dry multibilayers. In the former the helix axis lay parallel to the bilayer plane. In the latter the axis was parallel to the bilayer normal. The temperature was above the transition temperature and the results were relatively independent of the lipid employed. Huang and Wu (1991) have related helix orientation to $P:L$. If $P:L$ is below a critical value, most of the peptide molecules are parallel to the bilayer plane, regardless of the water content.

Overall it seems that the *average* orientation of amphipathic CFPS such as alamethicin and melittin is quite sensitive to the physical state of the bilayer. With dry bilayers or partially hydrated (30%) multilayers the helices partition into the bilayer phase, orienting themselves parallel to the bilayer normal. With fully hydrated single bilayers the helices lie parallel to the plane of the bilayer, at an interfacial location. If the bilayer is sufficiently hydrated then lowering the temperature below the transition temperature appears to force the helix out of the bilayer. Thus the free energy difference between the two orientations cannot be very large and one may expect that it can be perturbed by a change in transbilayer potential.

Peptide partition and aggregation in the bilayer

Schwarz et al. (1986) used CD measurements to study alamethicin incorporation into DOPC small unilamellar vesicles (SUVs), given that addition of SUVs to alamethicin changed the CD spectrum consistent with an increase in the percentage helicity. Alamethicin incorporation isotherms (i.e. plots of $r = [\textit{associated alamethicin}]/[\textit{lipid}]$ vs. $C = [\textit{free aqueous alamethicin}]$) thus derived exhibited two striking features. Firstly, the saturating value of $r\,(>0.4)$ is inconsistent with a alamethicin binding with its helix axis parallel to the bilayer surface, and so suggests incorporation of alamethicin into the bilayer *per se*. Secondly, C has to reach a critical concentration (C^*) before there is an upturn in the isotherm and the level of incorporated alamethicin rises steeply. This is suggestive of aggregation of alamethicin within the bilayer. Subsequent studies (Rizzo et al. 1987) investigated the dependence of C^* on temperature, ionic strength and lipid composition, and suggested a simple model in which monomeric alamethicin partitions into the bilayer and subsequently aggregates.

Studies on the kinetics of incorporation were carried by stopped-flow investigations of the interaction of fluorescence-labelled alamethicin with DOPC and DMPC SUVs (Schwarz et al. 1987). The results were analyzed in terms of the theoretical framework outlined by Schwarz (1987). Above the phase transition temperature of the bilayers, incorporation kinetics could be described by a single exponential function, i.e. consistent with an essentially one-step incorporation process. The rate constant for this process is quite high, somewhat below the rate for a diffusion-limited reaction. The authors interpreted this in terms of rapid incorporation of monomeric alamethicin into the bilayer, followed by a slower conformational change and alamethicin aggregation.

More detailed studies on the dependence of C^* on lipid composition (Stankowski et al. 1988; Stankowski and Schwarz 1989) provided further evidence for bilayer incorporation of alamethicin, rather than binding to the membrane surface. Binding isotherms were analyzed so as to separate out lipid effects on peptaibol incorporation and on subsequent aggregation. The former seemed to be sensitive to bilayer composition, whereas the latter did not. In particular, alamethicin incorporation was favoured by phosphatidylcholine headgroups, the absence of cholesterol, thin bilayers and saturated acyl chains. Furthermore, the CD measurements suggested that the conformation of incorporated alamethicin was sensitive to membrane thickness and lipid packing.

More recently, spin label ESR techniques have been used to probe alamethicin-bilayer interactions (Archer et al. 1991). Two nitroxide labelled derivatives, one consisting of alamethicin labelled at the C-terminus and another of *per*-(Aib→Leu)-Alm (see below) labelled at the N-terminus, were prepared. Both were shown to be monomeric in solution in methanol and at low concentrations in water. Their binding to lipid bilayers was cooperative, as in the studies of Schwarz and colleagues, suggesting aggregation within the bilayer. However, ESR spectra of both peptides over a wide range of $P:L$ ratios provided no evidence for peptide aggregation and were consistent with monomeric peptide. It is possible that the presence of the spin label prevents aggregation within the bilayer, but this seems unlikely as it was demonstrated that the spin-labelled derivatives formed ion channels in the presence of a transbilayer potential.

Electrical properties of peptaibol channels

The peptaibol CFPs, and alamethicin in particular, have been the subject of a wide range of electrical studies, providing a detailed understanding of ion channel properties and of the relationship between peptide structure and channel function. The following account of the functional properties of peptaibols is selective, with an emphasis on more recent investigations. Earlier investigations on alamethicin has been reviewed by Latorre and Alvarez (1981), and a more detailed account of the relationship between peptaibol sequence and channel function is provided by Boheim et al. (1987).

Macroscopic properties

Macroscopic studies of peptaibol induced bilayer conductance have provided valuable clues as to the mechanism of voltage activation of channels. The main experimental procedure has been to measure the steady-state conductance of a bilayer exposed on one face (the *cis* face) to an aqueous solution of alamethicin. By applying a slowly changing (typically, ca. 20 mV/s) voltage difference across the bilayer, a current-voltage ($I-V$) relationship may be determined (see Fig. 4). The $I-V$ relationship for alamethicin exhibits a marked asymmetry, with voltage-activation of alamethicin channels occurring principally at *cis* positive potentials. Vodyanoy et al. (1983) suggested that an *ideal* bilayer would show alamethicin induced current only at *cis* positive potentials, and that any current observed at elevated negative potentials is due to leakage of alamethicin through the bilayer. This was supported by the observation that increasing the dielectric constant of a bilayer, e.g. by employing di-bromostearyl PC as the bilayer lipid, resulted in a decrease in the asymmetry of the $I-V$ relationship.

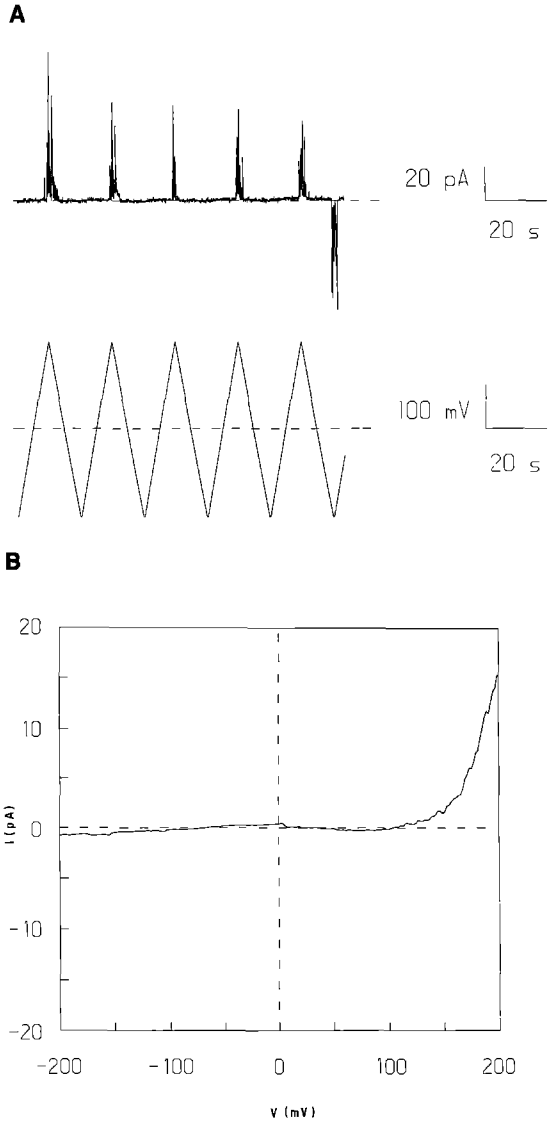

Fig. 4 A, B. Voltage activation of Alamethicin channels. **A** is taken from a recording made from a diphytanoyl phosphatidylcholine bilayer exposed to 0.5 μM Alm-R_f50 in the *cis* compartment. As shown in the lower trace, the transbilayer potential was a triangular wave of amplitude 200 mV and frequency 0.05 Hz. The resultant current is shown in the upper trace. **B** is the average current-voltage relationship derived from this data. It is evident that Alm channel activation occurs overwhelmingly at *cis* positive potentials. (Figures reprinted from Sansom (1991), Progr. Mol. Biophys. Mol. Biol. 55:139–236, with kind permission of Pergamon Press Ltd.)

The steady state conductance, $G = I/V$, of a bilayer exposed to alamethicin can be described by

$$G = \Gamma C^N \exp(V/V_e)$$

where Γ is a constant dependent on lipid composition and ionic strength, C is the concentration of alamethicin in the *cis* aqueous phase, N is the mean number of alamethicin monomers in channel complex and V_e is the voltage change required to give an e-fold increase in conductance. Furthermore, $V_e = kT/eN\alpha$ where k is the Boltzmann constant, T the temperature, e the electronic charge and α the effective gating charge. Thus, if a set of $I-V$ relationships is obtained for different alamethicin concentrations, C, it is possible to estimate N and α. In this manner, Hall et al. (1984) demonstrated that for a bacterial PE bilayer exposed to alamethicin in the presence of 1M KCl, $N = 10.5$ and $\alpha = 0.59$. This is consistent with alamethicin channels being formed by helix bundles of, *on average*, 10 or 11 monomers.

Hall et al. (1984) also analyzed the effect of bilayer thickness on the macroscopic $I-V$ relationships of alamethicin, using monoglyceride/squalene bilayers with different mono-unsaturated chains lengths. The effective gating charge per monomer, α, was largely independent of bilayer composition, but that the mean number of monomers per channel increased with the lipid chain length, from $N = 2$ for 14:1 lipid to $N = 11$ for 20:1 lipid. This is consistent with the helix bundle model in that the gating charge is a property of the monomer *per se*, whereas the mean number of helices in a bundle is sensitive to the physical properties of the lipid bilayer.

To investigate the mechanism of voltage activation of channels, Hall et al. (1984) examined the effects of systematic changes in the location of electrostatic charges on the alamethicin helix on $I-V$ relationships. A free negative charge close to the C-terminus (as in Alm-R_f30) or of a free positive charge at the N-terminus (achieved by removing the N-terminal acetyl group and blocking E18 of Alm-R_f30) resulted in an asymmetric $I-V$ relationship. In the former case, channels were activated at *cis* positive potentials, in the latter case at *cis* negative potentials. This may be explained in terms of a voltage activation mechanism which requires alignment of helix dipoles anti-parallel to the imposed field, with the presence of a free positive or negative charge anchoring one end of the helices at the *cis* face of the bilayer (see below). However, further results indicate that the gating mechanism may be somewhat more complex. In the above study, an alamethicin derivative with both the N-terminus and E18 blocked, i.e. a derivative lacking a free charge at either end of the helix, formed channels at both *cis* negative and *cis* positive potentials. However, Alm-R_f50, which also lacks any free charges, resembles Alm-R_f30 in that it is activated only at *cis* positive potentials (Fig. 4). Furthermore, the 16 residue peptaibol Zrv-IIB, which also lacks any charged sidechains, is activated only at positive potentials (Balaram et al. 1992). It therefore appears that either a free charge is not the only way to generate an "anchor" for one end of the peptide, or that a more complex mechanism of channel activation is involved.

Microscopic studies

Microscopic studies, i.e. investigations at the single channel level, have yielded much information about the properties of the open channel *per se*. Such data provide essential clues concerning the molecular structure of peptaibol channels. Gordon and Haydon (1972, 1975) demonstrated the most characteristic property of alamethicin channels, i.e. multi-level bursts of channel openings interspersed with prolonged closed periods (Fig. 5A, B). The frequency of occurrence of channel bursts (and hence the inter-burst closed intervals) is strongly dependent upon

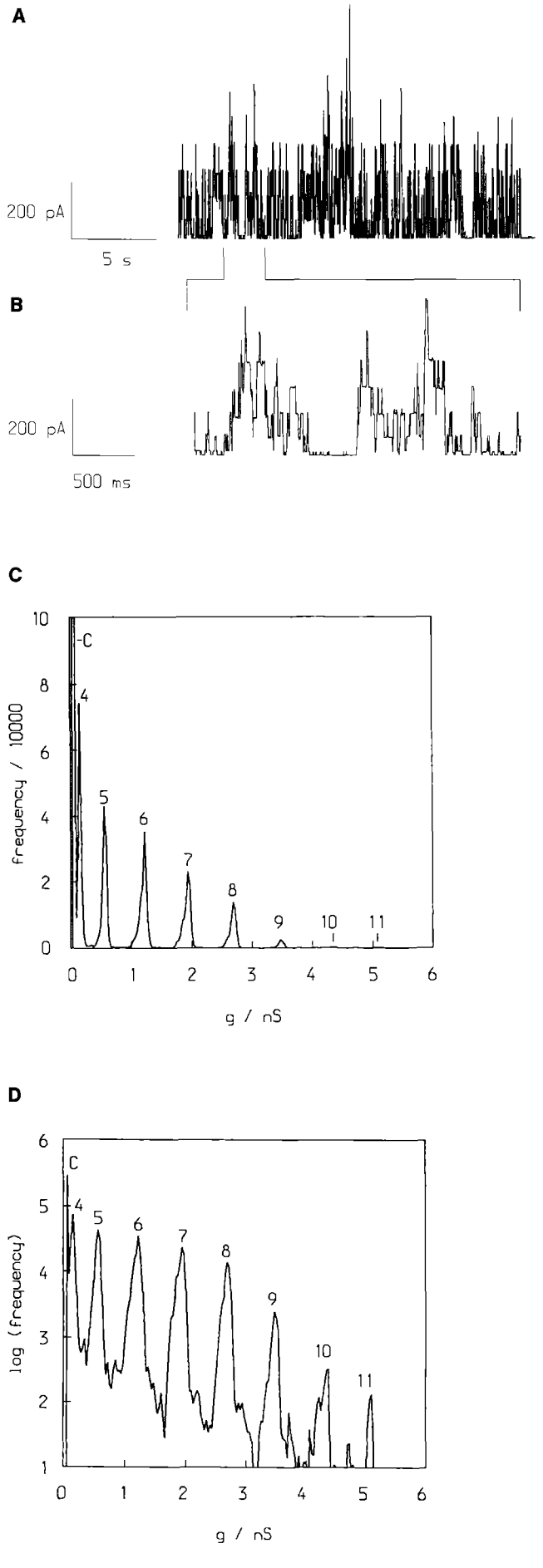

the trans-bilayer potential, providing a microscopic explanation of voltage activation of alamethicin conductance.

Conductance levels

The pattern of successive conductance levels within a single burst of multi-level openings of an alamethicin channel provides the best evidence for the helix bundle (or barrel-stave; Boheim et al. 1983) model of channel formation. A progression of conductance levels may be calculated using a simple equivalent-cylinder model for channel formation by helix bundles (Mellor and Sansom 1990; Sansom 1991; Balaram et al. 1992). In this, the channel is approximated by a cylindrical pore of length l and radius a which runs down the centre of a bundle of N helices, and is filled with electrolyte of resistivity ϱ. The conductance of such a pore (Hille 1992) is given by:

$$g = \frac{\pi a^2}{\varrho\,(l + \pi a/2)},$$

where the radius of the central pore is given by:

$$a = R\left[\frac{1}{\sin(\pi/N)} - 1\right].$$

Thus increasing the number of helices in the bundle increases the radius of the central pore and hence increases the conductance. An important prediction of this model of channel formation by peptaibols is that the conductance increment between successive levels, Δg_N, is not constant, but increases as the level, N, increases. Such a pattern of successive conductance levels is seen if one examines the experimental data (Gordon and Haydon 1972, 1975; Boheim 1974; Hanke and Boheim 1980; also see Fig. 5C, D). In particular, Δg_N increases as N increases. However, there is a quantitative discrepancy between the experimental data and the predictions of the model, in that observed conductances are somewhat less than the corresponding theoretical values (Sansom 1991). However, allowance should be made for the extreme simplicity of the model, which ignores possible ion/channel and ion/lipid interactions and oversimplifies the geometry of the pore. The degree of agreement provides convincing evidence for the helix bundle model.

Fig. 5A–D. Single Alamethicin channels. Single channel recording from a diphytanoyl phosphatidylcholine bilayer exposed to 0.25 μM Alm-R_f50 in the *cis* compartment, with 0.5 M KCl as the electrolyte and at a membrane potential of 125 mV. **A** shows multiple conductance level channel activity. **B** shows a section of the recording on an expanded timebase. Individual channel openings may be seen. **C** is a conductance histogram derived from the same recording. The numbers above the peaks indicate the values of N if one assumes that the lowest conductance level (88 pS) corresponds to $N=4$. **D** shows the same histogram on a semi-logarithmic plot and reveals the increasing step size from one conductance level to the next as N increases. (Figures reprinted from Sansom (1991). Progr. Mol. Biophys. Mol. Biol. 55:139–236, with kind permission of Pergamon Press Ltd.)

The agreement between the theoretical and observed conductance level patterns enables one to use this data to estimate the numbers of helices present in alamethicin bundles. For the experimental data presented in Fig. 5C, D, the lowest conductance level depicted is 88 pS (in 0.5 M KCl, which would be approximately equivalent to 180 pS in 1 M KCl). Hanke and Boheim (1980) measured a lower conductance level (19 pS) in 1 M KCl, which was proposed to correspond to a trimeric bundle of alamethicin molecules. Thus, for Fig. 5 the stoichiometry of alamethicin bundles ranges from $N=4$ to $N=11$. This compares well with the figure of $N=10$ to 11 obtained from analysis of macroscopic $I-V$ relationships (see above), given that the latter corresponds to a high degree of activation of alamethicin channels, in which higher conductance levels will predominate. The pore diameters for $N=3$, 4 and 11 are, respectively, 1.55, 4.14 and 25.5 Å, compared to 2.66 Å for the (Pauling) diameter of a K^+ ion. Thus, some distortion of the helix bundle must occur if the $N=3$ bundle acts as a channel. The $N=4$ bundle can clearly form a channel, but some degree of peptide-ion interaction will occur. At the other extreme, the $N=11$ bundle will act as a simple electrolyte-filled pore, and thus will not be ion selective.

Ion selectivity

Macroscopic studies have revealed that the conductance induced by alamethicin (and a range of analogues) is weakly selective for cations (Hall et al. 1984). At the single channel level, Hanke and Boheim (1980) obtained a selectivity sequence $K^+, Rb^+, Cs^+ > Na^+ > Li^+$ for the lowest (19 pS in 1 M KCl) conductance level, which was also shown to be impermeable to Ca^{2+} and to Cl^- ions. Higher conductance levels exhibit little, if any, selectivity (Gordon and Haydon 1975), suggesting that ions pass through in a fully hydrated state.

Kinetics

The helix bundle model of channel formation by alamethicin has also been tested against the kinetics of switching between conductance levels *within* bursts of channel openings. Examination of such bursts at high time resolution reveals that transitions are exclusively between adjacent levels, i.e. from level N transitions can be made either to level $N+1$ or to level $N-1$. Thus, as discussed by Boheim (1974), the gating mechanism for alamethicin may be represented by:

$$C \rightleftharpoons O_3 \rightleftharpoons O_4 \rightleftharpoons \ldots \rightleftharpoons O_M$$

where C represents the closed channel, O_N is an open channel bundle containing N helices, M is the maximum bundle size, and where the downwards and upwards transition rates from O_N are k_{N-1} and k_{N+1} respectively. Via a stochastic theory analysis (Ball and Sansom 1989) one may show that maximum likelihood estimators of the transition rates are:

$$k_{N\pm1} = F_{N\pm1} / T_N$$

where $F_{N\pm1}$ is the total number of transitions $N \rightarrow N\pm1$ and where T_N is the total time spent in state N. The corresponding standard deviation is given by

$$SD_{N\pm1} = k_{N\pm1} / \sqrt{F_{N\pm1}}$$

(Balaram et al. 1992).

Using the above and related methods, the kinetics of peptaibol single channel gating has been investigated (Boheim 1974; Balaram et al. 1992). Absolute values of the transition rate constants are sensitive to e.g. the lipid composition of the bilayer. However, general principles do emerge. The mean dwell time of Alm-R_f50 averaged across conductance levels O_4 to O_{11} (for channels in a diPhyPC bilayer at +125 mV in the presence of 0.5 M KCl) is 4.6 ms (Balaram et al. 1992). The upwards and downwards transition rates vary slightly with N. However, the dependence of $k_{N\pm1}$ on N is not marked, and values for the two extreme levels of a burst do not differ by more than about one order of magnitude at the most. Boheim (1974) demonstrated that the main voltage dependence of alamethicin channel gating lay in pore formation, i.e. the duration of the inter-burst intervals. There is only a weak dependence of intra-burst transition rates on voltage. This results in a small shift in the percentage occupancy within bursts to higher N as V is increased.

The ionic strength of the surrounding solutions has a profound effect on alamethicin intraburst kinetics. Boheim et al. (1983) showed that increased ionic strength (a) increased the mean lifetime of all conductance levels; and (b) preferentially stabilized the lower conductance levels. A similar effect has been seen for a dansylated derivative of trichotoxin-40 (an 18-mer analogue of alamethicin; Hanke et al. 1983). This effect of increased ionic strength is a result of the decreased Debye length. As the Debye length approaches the dimensions of the channel, charge-charge and dipole-dipole repulsions between monomers decrease, thus stabilizing helix bundles.

Synthetic alamethicin analogues

The relationship between peptaibol sequence and channel function has been probed systematically in a series of studies by Molle and co-workers (Molle et al. 1988, 1989, 1991; Duclohier et al. 1992) employing synthetic analogues of Alm (see Table 1). Analogue L1, in which all Aib residues are replaced by Leu, forms channels in a similar manner to alamethicin. In macroscopic $I-V$ experiments in POPC/DOPE/DPPS/Chol bilayers, channels are activated by *cis* positive potentials. Analysis of the concentration dependence of $I-V$ curves yielded estimates of $N=8$ and $\alpha=0.46$, i.e. similar values to those for alamethicin under comparable conditions. In single channel experiments, discrete bursts of multi-level openings are observed, with successive conductance levels similar to those for alamethicin. L1 exhibits a 5–10 fold shorter mean dwell times in the different conductance levels, i.e. switching between adjacent conductance levels within a burst is 5 to 10 times faster than for alamethicin.

Molle and co-workers tested whether the faster kinetics of L1 reflected a decreased length of the peptide (relative to alamethicin) resulting from replacement of regions of 3_{10} helix by α-helix (Molle et al. 1989). Two 21-mer derivatives were synthesised – LL1 and SL1. LL1 produced even more rapid switching between conductance levels, such that it became difficult to resolve individual transitions. Intraburst switching of SL1 was slower than for LL1 and L1, but still faster than for alamethicin. These studies demonstrate that there is *not* a straightforward relationship between peptaibol length and intraburst switching rate.

Analogues L2, L3 and L4 were employed to investigate the effects of variations in the C-terminal structure of peptaibols on channel properties (Molle et al. 1991). L1, L2, L3 and L4 all formed strongly voltage-activated channels with similar intraburst kinetics. Thus, neither substitution of a C-terminal alcohol for a C-terminal amide (L2), extension of the C-terminus by one residue (L3) nor deletion of an anionic sidechain (L4) substantially altered channel activation or intraburst kinetics. However, L4 did show lower single channel conductances than the other three analogues.

The effect of proline→alanine substitutions on channel formation have been studied using L2, L2-P2A and L2-P14A (see Table 1; Duclohier et al. 1992). Macroscopic and single channel properties of L2 and L2-P2A are similar; the latter exhibits a small increase (ca. 2 fold) in intraburst switching rates. L2-P14A is of particular interest: (*i*) in macroscopic $I-V$ studies it is strongly voltage activated, despite the absence of the proline-induced kink; (*ii*) in single channel studies intraburst switching of L2-P14A is ca. 7 times faster than that of L2; and (*iii*) single channel conductances of L2-P14A are ca. 30–50% those of L2. Thus the properties of the open channel are considerably altered by loss of the central kink from the peptaibol helix.

Zervamicins

The zervamicins are a family of 16 residue peptaibols which, in some respects, resemble other truncated analogues of alamethicin, e.g. the trichorzianines (19 residues, Molle et al. 1987; Duclohier et al. 1989). Zrv-IIB resembles alamethicin in that its macroscopic $I-V$ relationship is asymmetric, with channel activation occurring at *cis* positive potentials (Balaram et al. 1992). As discussed above, this is somewhat surprising given that Zrv-IIB has no charged sidechains and so might be expected to be activated equally at positive and negative potentials. Furthermore Zrv-IC, in which the glutamine at position 3 of Zrv-IIB is replaced by glutamate (Table 1), is activated by *cis* negative potentials. These results have important consequences with respect to mechanisms of peptaibol channel activation. They suggest that the hypothesis that charged residues anchor one end of the peptaibol helix to the bilayer-aqueous interface whilst the uncharged end is free to move into and out of the bilayer in response to changes in transbilayer potential may be somewhat too simplistic. Analysis of Zrv-IIB $I-V$ relationships vs. peptide concentrations yields an estimate of $N=14$ (in diPhyPC bilayers), i.e. somewhat higher than the corresponding value for alamethicin. Thus the shorter peptaibol forms larger N bundles. This has also been observed with certain 17 residue alamethicin analogues (Hall et al. 1984).

At the single channel level, Zrv-IIB produces bursts of multi-level openings. Conductance differences between successive levels, Δg_N, are higher than corresponding values for alamethicin. This is predicted by the equivalent cylinder model as the length of the pore (and hence its electrical resistance) is proportional to the length of the peptide. For the higher N values observed Δg_N values are less than those predicted by this model. This has also been observed for alamethicin (Boheim 1974). This may be explained by proposing that larger N bundles are distorted away from an ideal cylindrical cross-section towards a "torpedo" shape, i.e. the bundles are squashed within the plane of the membrane.

Maximum likelihood analysis of the kinetics of switching between adjacent conductance levels (see above) reveals this to be about 10 times faster for Zrv-IIB than for alamethicin. The rate constant for downwards transitions, $k_{N,N-1}$, is approximately independent of the level N, whereas the rate for upwards transitions, $k_{N,N+1}$, decreases as N increases (Balaram et al. 1992).

The synthetic apolar zervamicin derivative, Zrv-A1-16, also forms channels (Balaram et al. 1992). However, its limited solubility in water means that channels can only be observed if the peptaibol is dissolved directly in the lipid solution (in pentane) used to form bilayers. Voltage-activated channels are seen but, at a nominal $P:L$ of 1:100, only two conductance levels were observed, rather than the multi-level bursts typical of more polar peptaibols.

Overall, the zervamicins form channels comparable to those of other peptaibols. This is interesting, given the differences in conformation of the C-terminal helix between alamethicin and the zervamicins.

Modelling peptaibol channels

Voltage-dependent activation

Alternative models. Electrical studies of peptaibols demonstrate that voltage-activation results primarily from an increase in the number of bursts of multi-level channel openings as V is increased. There are several contending models to explain this increase (Fig. 6; also see Sansom 1991). These may be divided into three broad classes, and differ principally in the nature of the voltage dependent step.

Schwarz and coworkers (see e.g. Rizzo et al. 1987; Stankowski et al. 1988) have emphasized correlations between the effects of ionic strength, lipid composition etc. on alamethicin binding to lipid vesicles with the corresponding effects on steady state $I-V$ relationships. They proposed a mechanism in which *voltage-dependent* partition of alamethicin between the aqueous and bilayer phases occurs prior to *voltage-independent* aggregation of

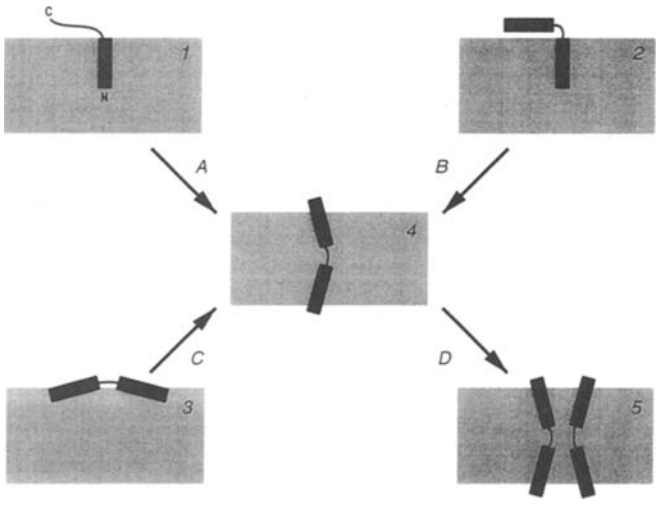

Fig. 6A–D. Voltage-gating models for peptaibol channels. 1, 2 and 3 show alternative possibilities for the disposition of peptaibol monomers (black) in the bilayer (grey) in the absence of a transbilayer voltage. 1 corresponds to the N-terminal segment of the monomer in a helical conformation and inserted into the bilayer, whilst the C-terminal segment is in an extended conformation. 2 corresponds to a peptaibol molecule with a pronounced kink between the two helices, with the N-terminal helix inserted in the bilayer whilst the C-terminal helix lies on the bilayer surface. 3 corresponds to the entire peptaibol molecule, with a relatively small kink angle, sitting on the bilayer surface. **A, B** and **C** are the voltage dependent transitions corresponding to 1, 2 and 3, resulting in a peptaibol monomer inserted into the bilayer (4). Monomers then aggregate within the plane of the bilayer (**D**) to form transbilayer helix bundles (5)

membrane bound peptide to form channels. There are, however, some problems with this model. In particular, the spectroscopic studies on which estimates of alamethicin partitioning into the bilayer were based were carried out at significantly higher $P:L$ ratios than the electrical measurements, and in the absence of a transbilayer potential. Also, the evidence of Archer and Cafiso (1991), using spin-labelled alamethicin to investigate partitioning into the bilayer of SUVs, fails to support voltage-dependent partitioning. Under conditions where all of the peptide was shown to be membrane bound, alamethicin was shown to induce transbilayer conductance in a voltage-dependent fashion.

The second class of model invokes a voltage-dependent conformational change in the alamethicin molecule (Fig. 6A, B). Hall et al. (1984) suggested a voltage dependent $\beta \rightarrow \alpha$ transition for the C-terminal region of the molecule, along with a "hinge-bending" movement to form a membrane-spanning helix (Fig. 6.4). A related model was proposed by Fox and Richards (1982) in which in the absence of a transbilayer voltage the N-terminal portion of the alamethicin molecule is inserted into the bilayer in a helical conformation. Imposing a voltage fully inserts the peptide molecule into the bilayer. Insertion is coupled with a conformational change in the C-terminal region of the molecule. Both of these models require conformational flexibility about the central proline residue. The C-terminal region, prior to the voltage-dependent transition, may exist either in a more extended conformation (Fig. 6.1) or in a helical conformation (Fig. 6.2). Aggregation of alamethicin molecules may occur prior to the conformational transition, as well as subsequent to formation of transbilayer helices (as in Fig. 6).

The third class of model suggests that alamethicin helices *reorient* relative to the bilayer in response to changes in transbilayer potential. There are three variants on this class of model. In the "flip-flop" model of Boheim et al. (1983) it is proposed that, when $V=0$, there are *anti-parallel* bundles of alamethicin helices traversing the bilayer (corresponding to closed channels). Upon imposing a voltage difference, those helices parallel to the field flip, resulting in the formation of *parallel* helix bundles (open channels) and of free monomeric helices. Addition of monomers to existing bundles forms higher conductance level channels. The model of Mathew and Balaram (1983 a, b) is similar in that it proposes a transition between anti-parallel and parallel helix bundles. However, it allows for expulsion of a central helix which otherwise occludes the pore and results in a closed channel aggregate. The third variant does not involve complete flip-flop of transbilayer helices (which might be expected to have a high activation energy) but rather reorientation from a state in which the helix axis is perpendicular to the bilayer normal, to one in which it is parallel to the normal (see e.g. Baumann and Mueller 1974; Alvarez and Latorre 1981). In this model surface bound alamethicin may aggregate to some extent prior to insertion into the bilayer. Again, multi-level channels result from addition/removal of monomeric units from the helix bundle.

Of these three classes of models, the conformational change and the helix reorientation models provide somewhat more plausible explanations of voltage activation at the molecular level. They will now be examined in detail.

Helix dipoles and helix reorientation

Several authors have discussed the possibility of a significant dipole moment associated with an α-helix (Wada 1976; Hol et al. 1978, 1981; Hol 1985). The helix dipole arises from alignment of the molecular dipoles associated with the peptide bond. The peptide bond dipole is 3.5 D (0.72 eÅ; 1.1×10^{-29} Cm), parallel to the O=C and H–N bonds. In an α-helix the peptide bond dipoles are aligned such that the overall dipole is approximately parallel to the helix axis and has a magnitude equal to 90–95% of the sum of the constituent peptide dipoles. For example, a 20 residue helix has an overall dipole of ca. 63 D. This is approximately equivalent to a partial charge of + ½ at the N-terminus and – ½ at the C-terminus of the helix. Note that the helix dipole arises solely from contributions of the peptide backbone, and is independent of any dipole arising from asymmetric distribution of charged side-chains along the length of the helix.

Molecular dipoles have been estimated experimentally for alamethicin and related peptaibols. Combined dielectric and ultracentrifugation measurements on alamethicin-R_f50 in octanol (Schwarz and Savko 1982a, b) suggest that in this environment alamethicin exists predominantly as an elongated monomer, of dimensions

13 Å by 35 Å, with a dipole of ca. 75 D running parallel to the long axis of the molecule. This is equivalent to a partial charge of ± 0.45 at each end of the molecule, and so is in reasonable agreement with predictions based on a simple α-helical model (also see below).

Molecular dipoles may also be calculated from atomic coordinates and partial charges. Such calculations thus incorporate both contributions from the helix dipole and from charged and polar sidechains. For alamethicin-R_f30 and -R_f50 and for zervamicins-IIB and -A1-16, using partial charges from the Charmm V21.3 force field, dipole moments of 141, 79, 64 and 56 D respectively are obtained. The values for Alm-R_f30 and -R_f50 reveal how substitution of Q18 for E18 residue at position 18 results in a substantial reduction of the dipole moment. Interestingly, the calculated value for Alm-R_f50 is very similar to the experimental estimate of Schwarz and Savko (1982a, b, above). This lends some confidence to the use of this model of Alm-R_f50 in further calculations.

Estimates of molecular dipoles may be compared with measurements of the gating charge per monomer, α, obtained from analysis of alamethicin $I-V$ relationships (see above). Assuming that upon reorientation the alamethicin molecule lies parallel to the field, and that the entire fall in electrostatic potential between the two faces of the bilayer occurs across the length of the helix, then for Alm-R_f30 ($\mu = 141$ D) the gating charge per monomer for helix reorientation is 0.97 and for Alm-R_f50 ($\mu = 79$ D) it is 0.54. These values compare favourably with the experimental estimates of Hall et al. (1984) for Alm-R_f30, which ranged from 0.48 to 0.94, depending upon the bilayer thickness. Such correspondence between the predicted and experimentally estimated gating charges is perhaps the strongest evidence in favour of the helix reorientation model.

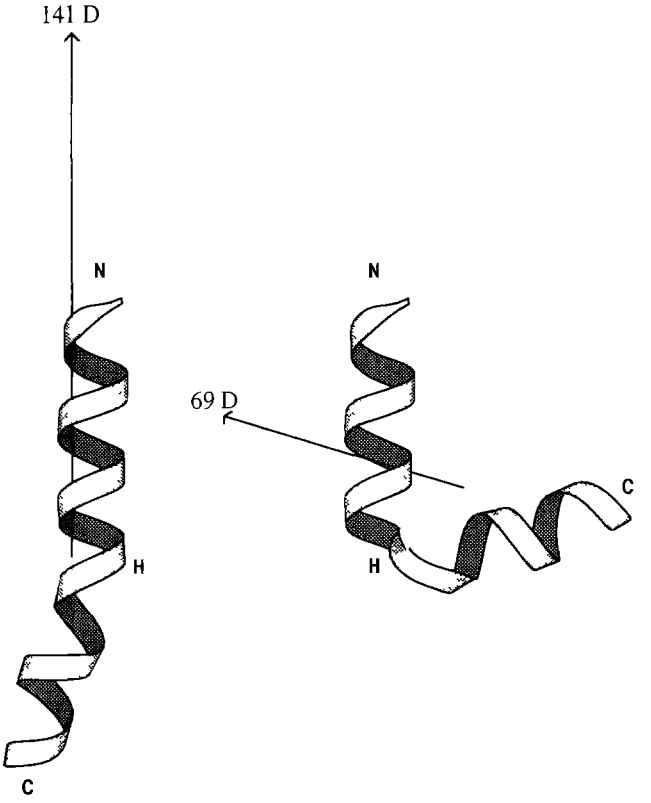

Fig. 7. "Hinge-bending" of peptaibol molecules. The left-hand structure represents Alm-R_f30 in the conformation seen in the crystal. The arrow indicates the magnitude and direction of the molecular dipole moment. The right-hand structure represents the "low dipole" conformation of Alm-R_f30 obtained via bending about a "hinge" (H) at residue G11 (see Table 2 and text for details)

Conformational changes

The major evidence in favour of a voltage-induced conformational change comes from the results of Brumfeld and Miller (1990 – see above). Two possible conformational changes require consideration: (*i*) a β-strand→α-helix transition of the C-terminal region of the molecule; and (*ii*) "hinge-bending" about the proline-induced kink altering the relative orientation of the N- and C-terminal helices.

There is little evidence in favour of a β→α transition in response to an applied electrostatic field. Early NMR studies suggested the possibility of β structure in the C-terminal half of the molecule (Bannerjee et al. 1983) and CD studies suggest changes in the percentage helicity of peptaibols as a function of solvent. However, there is no evidence for an extended β structure from more recent NMR studies or from crystallographic studies. Furthermore, the percentage helicity estimated from CD measurements made in the presence of phospholipid vesicles is consistent that in the crystal structure.

The evidence for hinge-bending changes in peptaibol conformation is more compelling. Although the crystal structure of alamethicin shows only small variations in kink angle, the zervamicin structures suggest that greater variation is possible. Extending such considerations to proline-containing helices in general, there is considerable variation in kink angles. Molecular dynamics studies (on alamethicin, melittin and helix-F of bacteriorhodopsin) suggest that hinge-bonding motion may occur on a ca. 10 pS timescale. However, this is not supported by NMR studies of dynamics, a discrepancy which remains to be resolved. Overall it would seem that changes in kink angle are possible, but the timescale of such transitions remains to be established.

Is the magnitude of the electrostatic field generated across a bilayer by a voltage difference of ca. 100 mV sufficient to induce a change in kink angle? One way of approaching this is to calculate the molecular dipole as a function of kink angle. This has been carried out in a simplified manner for Alm-R_f30 and -R_f50 (Sansom, unpublished results; see Fig. 7 and Table 2). The starting points were the crystal structure of Alm-R_f30, and the corresponding model (see above) of Alm-R_f50. Residue G11 was chosen as a simple "hinge" because its carbonyl oxygen does not form an intra-molecular H-bond, and because of the conformational flexibility of glycine. A simple grid search was performed, varying the backbone torsion angles in 20° increments. For each resultant structure the dipole moment and potential energy were calcu-

Table 2. Dipole moments and hinge bending

	Alm-R_f30		Alm-R_f50	
	high μ	low μ	high μ	low μ
(ϕ, ψ) of G11 (°)	(−73, −26)	(+80, −100)	(−71, −28)	(+160, +160)
kink angle (°)	38	78	44	55
E_V (kcal/mol)	−64	−32	−64	−61
E_E (kcal/mol)	−616	−611	−661	−636
μ (D)	141	69	79	43
$\Delta U/RT$	1.9		0.96	
P_{HIGH}/P_{LOW}	6.7		2.6	

E_V and E_E are the van der Waals and electrostatic energies, respectively, of the peptaibol molecules, calculated using Quanta and the Charmm V21.3 parameter set. ΔU is the difference in potential energy between the high and low μ forms of the molecule, with both forms of the molecule aligned parallel to a field of 3.3×10^7 Vm^{-1} (equivalent to a potential difference of 100 mV across a bilayer thickness of 3 nm). P_{HIGH}/P_{LOW} is the relatively probability of the high μ and low μ conformations, calculated using Boltzmann's equation and the value of ΔU tabulated

lated using Quanta and Charmm V21.3. The structures were sorted in order of dipole moment and those with unacceptably high potential energies excluded. For both R_f30 and R_f50 the highest dipole structure was very close to the corresponding crystal (or model) structure, and so the latter was employed as the "high μ" structure. The high μ and low μ structures are compared in Fig. 7 and Table 2. From Fig. 7 it is evident that the low μ structure is higly kinked (kink angle = 78°). From Table 2 it can be seen that G11 may adopt (at least) two alternative conformations to generate a low μ, highly kinked structure. In both cases the resultant (ϕ, ψ) values for G11 are within the observed range for glycine residues in highly refined protein structures (Richardson and Richardson 1989).

Using the estimated values of the dipole moments one may attempt to calculate the difference in potential energy of the high and low μ conformations when in an electrostatic field comparable to that across a lipid bilayer. For a field generated by a voltage drop of 100 mV across a distance of 3 nm (i.e. 3.3×10^7 Vm^{-1}), assuming that the alamethicin molecules orient themselves such that their dipoles are parallel to the field both before and after the conformational change, the results in Table 2 are obtained. For Alm-R_f30 a voltage difference of 100 mV will alter the conformational equilibrium by ca. 6 fold in favour of the high μ form, whereas for Alm-R_f50 there would be a change of ca. 3 fold. This is a rather small shift in the equilibrium between the two forms, but if subsequent aggregation within the bilayer was highly cooperative, it could be sufficient to account for at least a component of voltage-activation of alamethicin channels.

Overall, the balance of evidence seems to favour the helix reorientation model for alamethicin activation. However, the results of Brumfeld and Miller (1990) suggest that helix reorientation may be coupled to a change in alamethicin conformation. This conformational change is likely to include voltage-induced hinge bending.

Open channel structure

Molecular models. In addition to providing insights into possible mechanisms of voltage-activation, knowledge of the high resolution structures of several peptaibol molecules enables one to develop molecular models of open channels. Such models are molecular interpretations of the "barrel-stave" proposal of Boheim et al. (1983), which has been shown to provide a convincing explanation of the multiple conductance levels of peptaibol channels (see above). Molecular models of open channels may be used as the basis of e.g. electrostatics calculations, and the resultant predictions compared with experimentally determined channel properties.

Hall et al. (1984) described a barrel-stave model which incorporated their proposal for a $\beta \rightarrow \alpha$ transition upon channel activation. In this model the *closed* channel consists of an inner β-barrel formed by the C-terminal regions of the monomers, surrounded by an outer bundle of N-terminal helices. The *open* channel consists of a bundle of parallel helices, with the possibility of some β-structure in the C-terminal regions. This model for the open channel is similar to that proposed by Fox and Richards (1982) in which the open channel is formed by a bundle of $N = 8$ to *12* parallel helices surrounding a central pore. The monomers are packed such that their N-terminal helices are in close contact whilst their C-terminal helices diverge from the pore axis, resulting in a funnel-shaped pore with the wider mouth at the C-termini. This arrangement may enable the E18 residues to be sufficiently separated to overcome destabilising electrostatic repulsions. Analysis of the $N = 8$ bundle suggested stabilisation by an annulus of H-bonds formed by alternating Q7 and H_2O molecules. This is similar to the proposal of Mathew and Balaram (1983a, b) for channel stabilisation via such H-bonds. Furthermore, energy minimization studies (Furois-Corbin and Pullman 1988) suggest that Q7-Q7 H-bonds may stabilize pairing of parallel N-terminal helices of alamethicin and of the related peptaibol trichorzianine. Interestingly, recent CD studies of alamethicin in the presence of phospholipid bilayers (Woolley and Wallace 1993) provide evidence for helix-helix interactions between alamethicin monomers. The Fox and Richards model also suggests that, in addition to Q7, solvent exposed carbonyl residues of residues 10 and 11 form part of the pore lining. With respect to changes in channel conductance it is suggested that in addition to changes in N, changes in conformation of Q7 residues may be important.

Channel-ion interactions

Electrostatics calculations (Harvey 1989), based on molecular models of the open channel structure, can be used to look at possible interactions of peptaibol channels with ions. Such calculations are of interest given the observation of Hall et al. (1984) that alamethicin channels are *weakly* cation selective *regardless* of the presence or absence of charged sidechains in the alamethicin molecule. This suggests that the ion selectivity filter is *not*

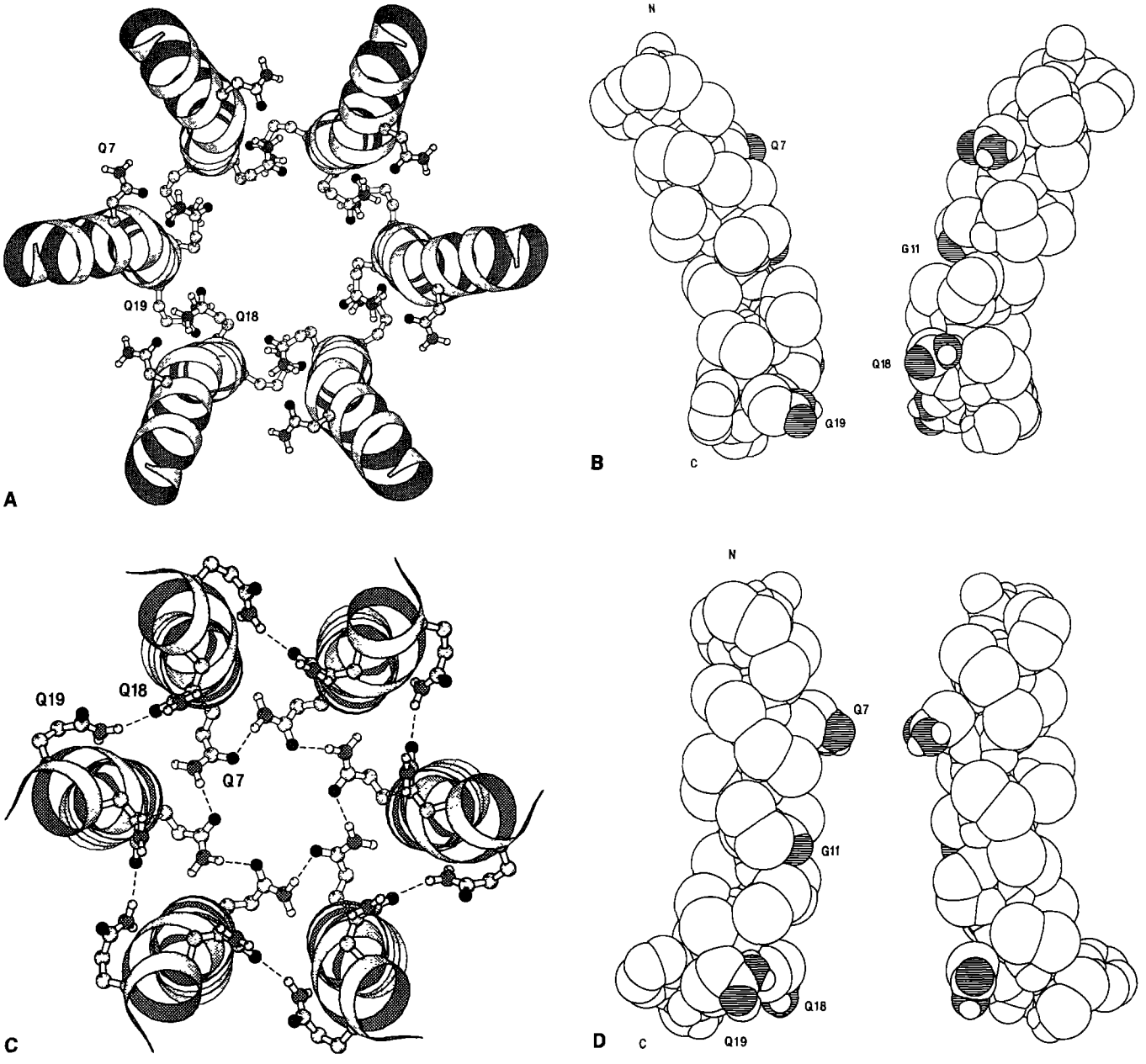

Fig. 8A–D. Models of Alm-R_f50 channels. **A** shows Model I for an $N=6$ bundle. The helices are packed with their C-terminal helical segments parallel. The view is from the N-terminal mouth of the channel. The sidechains of Q7, Q18 and Q19 are shown. The bundle is stabilized by H-bonds between the amide of Q19 and the C-terminal hydroxyl of the adjacent helix. **B** shows a space-filling representation of two opposite monomers of the same model, viewed down a perpendicular to the pore axis. The oxygens and nitrogens of the amide groups of Q7, Q18 and Q19, and the carbonyl oxygen of G11 are shaded. **C** shows Model II for an $N=6$ bundle. The helices are packed with their N-terminal helical segments parallel, and the model is viewed from the C-terminal mouth of the pore. Bundle-stabilizing hydrogen bonds involving residues Q7, Q18 and Q19 are shown as broken lines. **D** shows a space-filling representation of two opposite monomers of Model II, in the same manner as in **B**

composed of a ring of anionic E18 sidechains. To investigate this further, two groups of models of Alm-R_f50 bundles have been analyzed (Sansom, previously unpublished data) using similar methods to those described in Sansom et al. (1993). Alm-R_f50 was selected because the absence of an ionizable E18 residue removed concerns over local pK_As of carboxylic acid groups located within a transbilayer pore (see Edmonds 1989 for a discussion of some of the complexities of sidechain ionization *within* pores). As discussed above, the model of the Alm-R_f50 monomer was derived from the crystal structure of Alm-R_f30.

Model I (Fig. 8A, B) has the C-terminal helices packed parallel to one another, so as to form a funnel-shaped pore with the wider mouth at the N-terminal. Bundles with $N=4$ to 8 were constructed, with a C-terminal helix-helix separation of 9.5 Å and with the kinked helices oriented so that the convex (hydrophilic – see above) faces were directed towards the centre of the pore. The Q18 sidechains were "optimized" for cation trans-

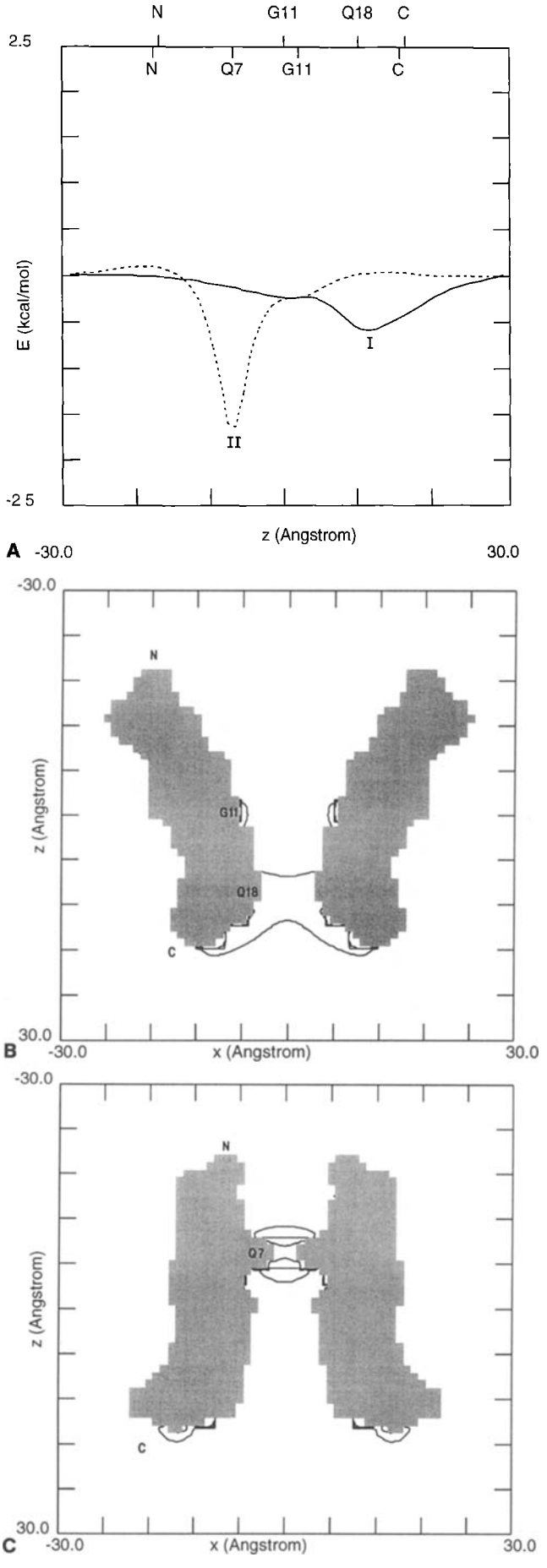

Fig. 9. **A** Electrostatic energy profiles for $N=6$ Alm-R_f50 channel models, calculated using $\varepsilon_{PROTEIN}=2$ and $\varepsilon_{SOLVENT}=78$, with an ionic strength of 500 mM. The solid line is the profile for a Model I channel, the dotted line is the profile for Model II. The approximate positions on z (the pore axis) of the N- and C-termini, of the amide groups of Q7 and Q18, and of the carbonyl oxygen of G11 are indicated at the top of the diagram. Downwards pointing ticks correspond to Model I, upwards pointing ticks to Model II. **B** and **C** are sections through $N=6$ Alm-R_f50 channel models (**B** – Model I; **C** – Model II). The grey polygons indicate the van der Waals envelopes of the peptaibol molecules. The solid lines are electrostatic energy contours, drawn at −1.5, −1.0 and −0.5 kcal/mol. Electrostatic energies were calculated in the same manner as for **A**

port (see Sansom 1992; Sansom et al. 1993) by energy minimization in the presence of an adjacent K^+ ion. The bundle is stabilized by van der Waals interactions between adjacent helices and by H-bonds from the sidechain of Q19 of one monomer to the terminal hydroxyl of the phenylalaninol of the adjacent monomer. From inspection of Fig. 8 B it is evident that the narrowest region of the pore is lined by the sidechains of Q18 and Q19, and by the exposed carbonyl oxygen of G11.

Model II (Fig. 8C, D) is the same as the Fox and Richards model in that the N-terminal helices are packed parallel to one another. Thus, the wider mouth of the pore is at the C-termini. Helix bundles, with an N-terminal helix-helix separation of 9.5 Å and the convex faces directed inwards, were generated using $N=4$ to 8 monomers. The bundles are stabilized by H-bonds between Q7 residues of adjacent monomers and also by Q18–Q19 H-bonds (Fig. 8C). The narrowest region of the pore is lined by the sidechain of Q7 and by the exposed carbonyl oxygen of G11 (Fig. 8D).

Potential energy calculations (Charmm V21.3) were used to evaluate the interaction energy at the monomer-monomer interface for the bundle models, defined by $E_{INT}=E_{DIMER}-2E_{MONOMER}$, where E_{DIMER} is the potential energy of a dimer taken from a bundle and $E_{MONOMER}$ is the energy of the corresponding monomer. For all values of N, interaction energies suggested that model II bundles were more stable than model I bundles. Also, for both models I and II, E_{INT} is largely independent of N, suggesting that stable bundles with differing numbers of monomer/bundle may be formed.

The electrostatic properties of these models have been investigated by solving the linearized Poisson-Boltzmann equation to obtain the electrostatic potential within the central pore. All electrostatics calculations were carried out using the UHBD program of Davis et al. (1991). The relative dielectric constants of the protein and solvent were 2 and 78 respectively, and the ionic strength equivalent to 500 mM KCl. A 1 Å grid was used throughout. Thus all volumes occupied by protein atoms are modelled as a low dielectric medium whereas all solvent-occupied volumes are modelled as electrolyte solutions with a Debye length of 4.3 Å. Clearly this will overestimate solvent and counterion screening of electrostatic interactions within the pore. However, given the relatively high con-

ductances of peptaibol channels, it provides a reasonable first approximation. Electrostatic potentials have been converted to energies by using a probe of charge +1. An electric field external to the pore molecule (e.g. the transbilayer potential) was not included in the calculations.

Electrostatic energy profiles for model I and model II $N=6$ bundles are shown in Fig. 9 A. These correspond to translation of the probe charge along the pore (i.e. z) axis. Corresponding sections through the models, with electrostatic energy contours and van der Waals envelope superimposed, are shown in Fig. 9 B, C. The energy profile for model I (C-terminal helices parallel) shows a major well corresponding to the position of the Q18 sidechains and a minor well corresponding to the carbonyl oxygen of G11. The energy profile for model II shows a somewhat deeper well at Q7 and again the well at G11. Examination of the sections through the pore confirms the origins of the potential wells. Thus, both models provide shallow electrostatic wells for a permeant cation. Note that in both cases the wells of the order of RT which is consistent with the relatively high conductance (ca. 1 nS) of the $N=6$ alamethicin channel.

Overall, it would seem that both model I and model II explain some of the electrical properties of alamethicin pores. Consideration of possible inter-helix H-bonds favours model II for the open channel. Model II would also be favoured for Alm-R_f30 in that it enables the charged E18 residues to remain at a reasonable separation from one another. For example, in the R_f50 models discussed above the separation of Cδ:18 atoms of adjacent monomers is 6.5 Å for model I compared with 8.0 Å for model II. Further evidence for model II arises from the studies of Molle et al. (1991) on synthetic alamethicin analogues. L4 (see Table 1) differs from L3 in deletion of the ionized E18 residue. This deletion results in a rather small (only 80%) reduction in single channel conductances. This suggests that interactions of permeant ions with E18 are weak, which is more consistent with model II in which these sidechains are found at the wider mouth of the pore. However, these considerations are not conclusive. It is possible that more detailed modelling studies will provide a solution to this problem.

Zervamicin channels

Molecular modelling studies and (somewhat simpler) electrostatics calculations have been carried out for zervamicin-IIB helix bundles (Sansom et al. 1993) with $N=4$ to 8 parallel helices surrounding a central pore. For this peptaibol it was found to be more energetically favourable to pack the monomers with their C-terminal helical segments in close contact. The resultant bundles were stabilized by hydrogen bonds between glutamine 11 and hydroxyproline 10 of adjacent helices. Interaction energy profiles (*in vacuo*) for movement of three different probes species (K^+, Cl^- and water) through the central pore where analyzed. The conformations of: (a) the sidechain of glutamine 3; (b) the hydroxyl group of hydroxyproline 10; and (c) the C-terminal hydroxyl group were independently "optimized" in order to maximize favourable interactions between the channel and the probes, resulting in favourable interaction energy profiles for all three. This suggests that conformational flexibility of polar sidechains may enable the channel lining to mimic an aqueous environment, and helps to explain why peptaibol channels are only *weakly* ion selective.

Conclusions

What then do we know concerning peptaibols and their ion channels? From crystallographic and spectroscopic studies it is clear that peptaibols form amphipathic helices when in a membrane-like environment, and that these helices are kinked in the region of the central proline residue. This provides a firm basis on which to model the structures of further peptaibols. Concerning the nature of interactions of peptaibols with bilayers, there is a degree of consensus that orientations both perpendicular to and parallel to the bilayer plane may be adopted, at least in the absence of an applied transbilayer potential. The aggregation state of peptaibols when interacting with bilayers is less certain. Finally, there now exists a wealth of experimental data on the ion channel properties of peptaibols. This enables detailed comparisons to be made with the channel properties of novel synthetic peptaibols and derivatives.

There are three areas in which significant progress seems likely in the near future. Firstly, more information is required on the dynamics of peptaibols in different environments. Both experimental and simulation studies will contribute to such investigations, and the results will be of importance in the second area, that of the mechanism of voltage activation of peptaibol channels. Spectroscopic and molecular dynamics studies of peptaibol conformations *in the presence of an externally imposed electrostatic field will* be needed to address the latter problem. The third area of enquiry is in determining the structure of peptaibol helix bundles. This will enable detailed investigations of channel-ion interactions and calculation of free energy profiles for permeant ions (Åqvist and Warshel 1989).

Finally, one should reflect on the relevance of peptaibols to ion channels in general. A molecular understanding of the transitions underlying voltage gating of Na^+, K^+ and Ca^{2+} channels will require application of the experimental and computational methods currently being developed to investigate voltage activation of alamethicin. Studies of mechanisms of helix insertion into bilayers will prove invaluable in understanding the modes of action of channel-forming toxins such as colicin (Parker et al. 1989) and *Bacillus thuringiensis* δ-endotoxin (Li et al. 1991). As well as stimulating development of methodologies, general principles are emerging from investigations of peptaibol channels which may apply to channel and other transport proteins. Studies of helix bundle formation and of the interactions of ions with flexible, hydrophilic sidechains may prove of particular importance in this wider context.

Acknowledgements. This work was supported by a grant from the Wellcome Trust My thanks to J. Breed, I. D. Kerr, I. R. Mellor and R. Sankararamakrishnan for their contributions to work reported in this article.

References

Aléman C, Subirana JA, Perez JJ (1992) A molecular mechanical study of the structure of poly(α-aminoisobutyric acid). Biopolymers 32:621–631

Aqvist J, Warshel A (1989) Energetics of ion permeation through membrane channels: solvation of Na^+ by gramicidin A. Biophys J 56:171–182

Archer SH, Cafiso DS (1991) Voltage-dependent conductance for alamethicin in phospholipid vesicles: a test for the mechanism of gating. Biophys J 60:380–388

Archer SJ, Ellena JF, Cafiso DS (1991) Dynamics and aggregation of the peptide ion channel alamethicin: measurement using spin-labeled peptides. Biophys J 60:389–398

Balaram P (1992) Non-standard amino acids in peptide design and protein engineering Curr Opin Struct Biol 2:845–851

Balaram P, Sukumar M, Krishna K, Mellor IR, Sansom MSP (1992) The properties of ion channels formed by zervamicins. Eur Biophys J 21:117–128

Balasubramanian TM, Kendrick NCE, Taylor M, Marshall GR, Hall JE, Vodyanoy I, Reusser F (1981) Synthesis and characterisation of the major component of alamethicin. J Am Chem Soc 103:6127–6132

Ball FG, Sansom MSP (1989) Single channel gating mechanisms: model identification and parameter estimation. Proc R Soc London Ser B 236:385–416

Banerjee U, Tsui FP, Balasubramanian TN, Marshall GR, Chan SI (1983) Structure of alamethicin in solution: one- and two-dimensional ^1H NMR studies at 500 MHz. J Mol Biol 165:757–775

Banerjee U, Zidovetski R, Birge RR, Chan SI (1985) Interaction of alamethicin with lecithin bilayers: a ^{31}P and ^2H NMR study. Biochemistry 24:7621–7627

Barlow DJ, Thornton JM (1988) Helix geometry in proteins J Mol Biol 201:601–619

Baumann G, Mueller P (1974) A molecular model of membrane excitability. J Supramol Struct 2:538–557

Bogusz S, Boxer A, Busath DD (1992) An SS1-SS2 β-barrel structure for the voltage-activated potassium channel. Prot Eng 5:285–293

Boheim G (1974) Statistical analysis of alamethicin channels in black lipid membranes. J Membr Biol 19:277–303

Boheim G, Hanke W, Jung G (1983) Alamethicin pore formation: voltage-dependent flip-flop of α-helix dipoles. Biophys Struct Mech 9:181–191

Boheim G, Gelfert S, Jung G, Menestrina G (1987) α-Helical ion channels reconstituted into planar bilayers. In: Yagi K, Pullman B (eds) Ion transport through membranes. Academic Press, Tokyo, pp 131–145

Brumfeld V, Miller IR (1990) Electric field dependence of alamethicin channels. Biochim Biophys Acta 1024:49–53

Burgess AW, Leach SJ (1973) An obligatory alpha-helical amino acid residue. Biopolymers 12:2599–2605

Cascio M, Wallace BA (1988) Conformation of alamethicin in phospholipid vesicles: implications for insertion models. Proteins: Struct Funct Genet 4:89–98

Cowan SW, Schirmer T, Rummel G, Steiert M, Ghosh R, Pauptit RA, Jansonius JN, Rosenbusch JP (1992) Crystal structures explain functional properties of two *E. coli* porins. Nature 358:727–733

Davis ME, Madura JD, Luty BA, McCammon JA (1991) Electrostatics and diffusion of molecules in solution: simulations with the University of Houston Brownian Dynamics program. Comp Phys Commun 62:182–197

Dempsey CE (1990) The actions of melittin on membranes. Biochim Biophys Acta 1031:143–161

Dempsey CE, Bazzo R, Harvey TS, Syperek I, Boheim G, Campbell ID (1991) Contribution of proline-14 to the structure and actions of melittin. FEBS Lett 281:240–244

Duclohier H, Molle G, Spach G (1989) The influence of the trichozianin C-terminal residues on the ion channel conductance in lipid bilayers. Biochim Biophys Acta 987:133–136

Duclohier H, Molle G, Dugast JY, Spach G (1992) Prolines are not essential residues in the "barrel-stave" model for ion channels induced by alamethicin analogues. Biophys J 63:868–873

Durrell SR, Guy HR (1992) Atomic scale structure and functional models of voltage-gated potassium channels. Biophys J 62:238–250

Edmonds DT (1989) A kinetic role for ionizable sites in membrane channel proteins. Eur Biophys J 17:113–119

Esposito G, Carver JA, Boyd J, Campbell ID (1987) High resolution ^1H NMR study of the solution structure of alamethicin. Biochemistry 26:1043–1050

Fox RO, Richards FM (1982) A voltage-gated ion channel model inferred from the crystal structure of alamethicin at 1.5 Å resolution. Nature 300:325–330

Fraternali F (1990) Restrained and unrestrained molecular dynamics simulations in the NVT ensemble of alamethicin. Biopolymers 30:1083–1099

Frey S, Tamm LK (1991) Orientation of melittin in phospholipid bilayers: a polarized attenuated total reflection infrared study. Biophys J 60:922–930

Furois-Corbin S, Pullman A (1988) Conformation and pairing properties of the N-terminal fragments of trichorzianine and alamethicin: a theoretical study. Biochim Biophys Acta 944:399–413

Gordon LGM, Haydon DA (1972) The unit conductance channel of alamethicin. Biochim Biophys Acta 255:1014–1018

Gordon LGM, Haydon DA (1975) Potential-dependent conductances in lipid membranes containing alamethicin. Philos Trans R Soc London B 270:433–447

Hall JE, Vodyanoy I, Balasubramanian TM, Marshall GR (1984) Alamethicin: a rich model for channel behaviour. Biophys J 45:233–247

Hanke W, Boheim G (1980) The lowest conductance state of the alamethicin pore. Biochim Biophys Acta 596:456–462

Hanke W, Methfessel C, Wilmsen HU, Katz E, Jung G, Boheim G (1983) Melittin and a chemically modified trichotoxin form alamethicin-type multi-state pores. Biochim Biophys Acta 727:108–114

Haris PI, Chapman D (1988) Fourier transform infrared spectra of the polypeptide alamethicin and a possible structural similarity with bacteriorhodopsin. Biochim Biophys Acta 943:375–380

Harvey SC (1989) Treatment of electrostatic effects in macromolecular modelling. Proteins: Struct Funct Genet 5:78–92

Hille B (1992) Ionic channels of excitable membranes (2nd edn). Sinauer Associates, Sunderland, Mass

Henderson R, Baldwin JM, Ceska TA, Zemlin F, Beckmann E, Downing KH (1990) Model for the structure of bacteriorhodopsin based on high-resolution electron cryo-microscopy. J Mol Biol 213:899–929

Hol WG, Duijen PT von, Berendsen HJC (1978) The α-helix dipole and the properties of proteins. Nature 273:443–446

Hol WGL (1985) Effects of the α-helix dipole upon the functioning and structures of proteins and peptides. Adv Biophys 19:133–165

Hol WGL, Halie LM, Sander C (1981) Dipoles of the α-helix and β-sheet: their role in protein folding. Nature 294:532–536

Huang HW, Wu Y (1991) Lipid-alamethicin interactions influence alamethicin orientation. Biophys J 60:1079–1087

Kaback HR, Bibi E, Roepe PD (1990) β-Galactosidase transport in *E. coli:* a functional dissection of the *lac* permease. TIBS 15:309–314

Karle IL (1992) Folding, aggregation and molecular recognition in peptides. Acta Crystallogr B 48:341–356

Karle IL, Balaram P (1990) Structural characteristics of α-helical peptide molecules containing Aib residues. Biochemistry 29:6747–6756

Karle IL, Flippen-Andersen J, Sukumar M, Balaram P (1987) Conformation of a 16-residue zervamicin IIA analog peptide containing 3 different structural features: 3_{10}-helix, α-helix and β-bend ribbon. Proc Natl Acad Sci, USA 84:5087–5091

Karle IL, Flippen-Andersen J, Agarwalla S, Balaram P (1991) Crystal structure of Leu-zervamicin, a membrane ion channel peptide. Implications for gating mechanisms. Proc Natl Acad Sci, USA 88:5307–5311

Karle IL, Flippen-Andersen J, Agarwalla S, Balaram P (1992) Implications for a ion channel in Leu-zervamicin. In: Sarma RH, Sarma MH (eds) Crystal structure of polymorph B. Structure and Function. Vol 2 Proteins, New York, Academic Press

Kelsh LP, Ellena JP, Cafiso DS (1992) Determination of the molecular dynamics of alamethicin using ^{13}C NMR: implications for the mechanism of gating of a voltage-dependent channel. Biochimistry 31:5136–5144

Latorre R, Alvarez O (1981) Voltage-dependent channels in planar lipid bilayer membranes. Physiol Rev 61:77–150

Lear JD, Wasserman ZR, DeGrado WF (1988) Synthetic amphiphilic peptide models for protein ion channels. Science 240:1177–1181

LeBars M, Bachet B, Mornon JP (1988) Structure of a helical 19 peptide (trichorzianine AIIIC). Modelling of transmembrane channels. Z Kristallogr 185:588 (abstract)

Li J, Carroll J, Ellar DJ (1991) Crystal structure of insecticidal δ-endotoxin from *Bacillus thuringiensis* at 2.5 Å resolution. Nature 353:815–821

Marger MD, Saier MH (1993) A major superfamily of transmembrane facilitators that catalyse uniport, symport and antiport. TIBS 18:13–20

Marshall GD, Hodgkin EE, Langs DA, Smith GD, Zabrocki J, Leplawy MT (1990) Factors governing helical preference of peptides containing multiple α,α-dialkyl amino acids. Proc Natl Acad Sci, USA 87:487–491

Mathew MK, Balaram P (1983a) A helix dipole model for alamethicin and related transmembrane channels. FEBS Lett 157:1–5

Mathew MK, Balaram P (1983b) Alamethicin and related channel forming polypeptides. Mol Cell Biochem 50:47–64

Mellor IR, Sansom MSP (1990) Ion channel properties of mastoparan, a 14 residue peptide from wasp venom, and of MP3, a 12 residue analogue. Proc R Soc London B 239:383–400

Mellor IR, Thomas DH, Sansom MSP (1988) Properties of ion channels formed by *Staphylococcus aureus* δ-toxin. Biochim Biophys Acta 942:280–294

Miller C (1992) Hunting for the pore of voltage-gated channels. Curr Biol 2:573–575

Molle G, Duclohier H, Spach G (1987) Voltage-dependent and multi-state ionic channels induced by trichorzianines, anti-fungal peptides related to alamethicin. FEBS Lett 224:208–212

Molle G, Dugast JY, Duclohier H, Spach G (1988) Conductance properties of des-Aib-Leu-des-Pheol-Phe-alamethicin in planar lipid bilayers. Biochim Biophys Acta 938:310–314

Molle G, Duclohier H, Dugast JY, Spach G (1989) Design and conformation of non-Aib synthetic peptides enjoying alamethicin-like ionophore activity. Biopolymers 28:273–283

Molle G, Duclohier H, Julien S, Spach G (1991) Synthetic analogues of alamethicin: effect of C-terminal residue substitutions and chain length on the ion channel lifetimes. Biochim Biophys Acta 1064:365–369

Oiki S, Madison V, Montal M (1990) Bundles of amphipathic transmembrane α-helices as a structural motif for ion-conducting channel proteins: studies on sodium channels and acetylcholine receptors. Proteins: Struct Funct Genet 8:226–236

Padley RC, Cook JC, Rinehart KL (1977) High resolution and field desorption mass spectrometry studies and revised structures of alamethicins I and II. J Am Chem Soc 99:8469–8483

Parker MW, Pattus F, Tucker AD, Tsernoglou D (1989) Structure of the membrane-pore-forming fragment of colicin-A. Nature 337:93–96

Pastore A, Harvey TS, Dempsey CE, Campbell ID (1989) The dynamic properties of melittin in solution – investigation by NMR and molecular dynamics. Eur Biophys J 16:363–367

Rebuffat S, Prigent Y, Auvin-Guette C, Bodo B (1991) Tricholongins BI and BII, 19-residue peptaibols from *Trichoderma longibrachiatum*: solution structure from two-dimensional NMR spectroscopy. Eur J Biochem 210:661–674

Richardson JS, Richardson DC (1989) Principles and patterns of protein conformation. In: Fasman GD (ed) Prediction of protein structure and the principles of protein conformation, Plenum, New York, pp 1–98

Rizzo V, Stankowski S, Schwarz G (1987) Alamethicin incorporation in lipid bilayers: a thermodynamic analysis. Biochemistry 26:2751–2759

Sankararamakrishnan R, Vishveshwara S (1992) Geometry of proline-containing alpha-helices in proteins. Int J Peptide Protein Res 39:356–363

Sankararamakrishnan R, Vishveshwara S (1993) Characterisation of proline-containing α-helix (helix F model of bacteriorhodopsin) by molecular dynamics studies. Proteins: Struct Funct Genet 15:26–41

Sansom MSP (1991) The biophysics of peptide models of ion channels. Prog Biophys Mol Biol 55:139–236

Sansom MSP (1992) An investigation of the role of serine and threonine sidechains in ion channel proteins. Eur Biophys J 21:281–298

Sansom MSP (1993) Peering down a pore. Curr Biol 3:239–241

Sansom MSP, Kerr ID (1993) Influenza virus M_2 protein: a molecular modelling study of the ion channel. Prot Eng 6:65–74

Sansom MSP, Kerr ID, Mellor IR (1991) Ion channels formed by amphipathic helical peptides – a molecular modelling study. Eur Biophys J 20:229–240

Sansom MSP, Balaram P, Karle IL (1993) Molecular modelling of ion channels formed by zervamicin-IIB. Eur Biophys J 21:369–383

Schwarz G (1987) Basic kinetics of binding and incorporation with supramolecular aggregates. Biophys Chem 26:163–169

Schwarz G, Savko P (1982a) Dielectric probe of the electric-field-sensitive peptide alamethicin. Bioelectromagnetics 3:25–28

Schwarz G, Savko P (1982b) Structural and dipolar properties of the voltage-dependent pore former alamethicin in octanol/dioxane. Biophys J 39:211–219

Schwarz G, Savko P, Jung G (1983) Solvent-dependent structural features of the membrane active peptide trichotoxin A40 as reflected in its dielectric dispersion. Biochim Biophys Acta 728:419–428

Schwarz G, Stankowski S, Rizzo V (1986) Thermodynamic analysis of incorporation and aggregation in a membrane: application to the pore-forming peptide alamethicin. Biochim Biophys Acta 861:141–151

Schwarz G, Gerke H, Rizzo V, Stankowski S (1987) Incorporation kinetics in a membrane, studied with the pore-forming peptide alamethicin. Biophys J 52:685–692

Stankowski S, Schwarz G (1989) Lipid dependence of peptide-membrane interactions: bilayer affinity and aggregation of the peptide alamethicin. FEBS Lett 250:556–560

Stankowski S, Schwarz UD, Schwarz G (1988) Voltage-dependent pore activity of the peptide alamethicin correlated with incorporation in the membrane: salt and cholesterol effects. Biochim Biophys Acta 941:11–18

Stroud RM, McCarthy MP, Shuster M (1990) Nicotinic acetylcholine receptor superfamily of ligand gated ion channels. Biochemistry 29:1107–1123

Toniolo C, Benedotti E (1991) The polypeptide 3_{10}-helix. Trends Biochem Sci 16:350–353

Toyoshima C, Unwin N (1988) Ion channel of acetylcholine receptor reconstructed from images of post-synaptic membranes. Nature 336:247–250

Unwin N (1989) The structure of ion channels in membranes of excitable cells. Neuron 3:665–676

Unwin N (1993) Nicotinic acetylcholine receptor at 9 Å resolution. J Mol Biol 230:1101–1124

Vodyanoy I, Hall JE, Balasubramanian TM (1983) Alamethicin-induced current-voltage curve asymmetry in lipid bilayers. Biophys J 42.71–82

Vogel H (1987) Comparison of the conformation and orientation of alamethicin and melittin in lipid membranes. Biochemistry 26:4562–4572

Wada A (1976) The α-helix as an electric macro-dipole. Adv Biophys 9:1–63

Weiss MS, Kreusch A, Schiltz E, Nestel U, Welte W, Weckesser J, Schulz GE (1991) The structure of porin from *Rhodobacter capsulatus* at 1.8 Å resolution. FEBS Lett 280:379–382

Wine JJ (1993) Ion channels and transmembrane transporters. Curr Biol 3.118–120

Woolley GA, Wallace BA (1992) Model ion channels: gramicidin and alamethicin. J Membr Biol 129:109–136

Woolley GA, Wallace BA (1993) Temperature-dependence of the interaction of alamethicin helices in membranes. (submitted for publication)

Yee AA, O'Neil JDJ (1992) Uniform ^{15}N labeling of a fungal peptide: the structure and dynamics of an alamethicin by ^{15}N and ^{1}H NMR spectroscopy. Biochemistry 31:3135–3143